iScience

CellPress
OPEN ACCESS

Article

The BNT162b2 mRNA vaccine demonstrates reduced age-associated T_H1 support *in vitro* and *in vivo*

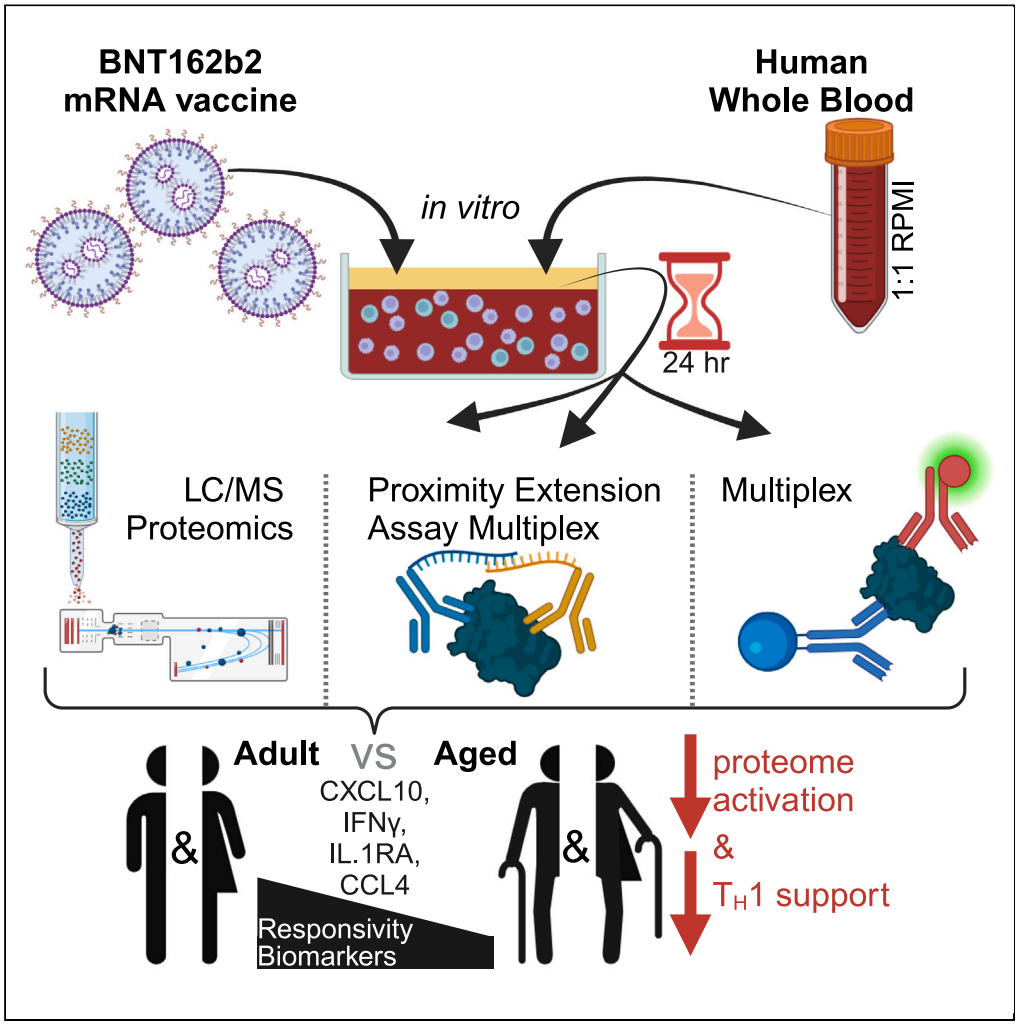

Byron Brook, Abhinav Kumar Checkervarty, Soumik Barman, ..., Hanno Steen, David J. Dowling, Ofer Levy

david.dowling@childrens.harvard.edu (D.J.D.)
ofer.levy@childrens.harvard.edu (O.L.)

Highlights

mRNA vaccine innate immunogenicity was modeled in human whole blood *in vitro*

Older adults had distinct, primarily lower T_H1, mRNA vaccine immune activation

Induction of CXCL10, IL-1RA, IFNγ, and CCL4 was reduced with age

In vivo mRNA vaccination in aged mice demonstrated impaired T_H1 immunity

Brook et al., iScience *27*, 111055
November 15, 2024
https://doi.org/10.1016/j.isci.2024.111055

iScience

CellPress
OPEN ACCESS

Article

The BNT162b2 mRNA vaccine demonstrates reduced age-associated T_H1 support *in vitro* and *in vivo*

Byron Brook,[1,2] Abhinav Kumar Checkervarty,[1,3,4] Soumik Barman,[1,2] Cali Sweitzer,[1] Anna-Nicole Bosco,[1] Amy C. Sherman,[1,5] Lindsey R. Baden,[5] Elena Morrocchi,[1,2,6] Guzman Sanchez-Schmitz,[1,2] Paolo Palma,[6,7] Etsuro Nanishi,[1,2] Timothy R. O'Meara,[1] Marisa E. McGrath,[8] Matthew B. Frieman,[8] Dheeraj Soni,[9] Simon D. van Haren,[1,2] Al Ozonoff,[1,2,10] Joann Diray-Arce,[1,2] Hanno Steen,[1,11] David J. Dowling,[1,2,12,*] and Ofer Levy[1,2,10,12,13,*]

SUMMARY

mRNA vaccines demonstrate impaired immunogenicity and durability in vulnerable older populations. We hypothesized that human *in vitro* modeling and proteomics could elucidate age-specific mRNA vaccine actions. BNT162b2-stimulation changed the plasma proteome of blood samples from young (18-50Y) and older adult (≥60Y) participants, assessed by mass spectrometry, proximity extension assay, and multiplex. Young adult up-regulation (e.g., PSMC6, CPN1) contrasted reduced induction in older adults (e.g., TPM4, APOF, APOC2, CPN1, PI16). 30–85% lower T_H1-polarizing cytokines and chemokines were induced in elderly blood (e.g., IFNγ, CXCL10). Analytes lower in older adult samples included human *in vivo* mRNA immunogenicity biomarkers (e.g., IFNγ, CXCL10, CCL4, IL-1RA). BNT162b2 also demonstrated reduced $CD4^+$ T_H1 responses in aged vs. young adult mice. Our study demonstrates the utility of human *in vitro* platforms modeling age-specific mRNA vaccine immunogenicity, highlights impaired support of T_H1 polarization in older adults, and provides a rationale for precision mRNA vaccine adjuvantation to induce greater immunogenicity.

INTRODUCTION

Severe acute respiratory syndrome coronavirus 2 (SARS-CoV-2) mRNA vaccines were rapidly developed, authorized, approved, and implemented to address the public health threat of coronavirus disease 2019 (COVID-19). Initial reports suggested a high vaccine efficacy (VE) of ~90–95% for BNT162b2 (*Comirnaty, Pfizer-BioNTech*) and mRNA-1273 (*Spikevax, Moderna*) in reducing severe COVID,[1,2] (compared to other respiratory viruses, e.g., yearly influenza VE of 10–80%[3,4]). While mRNA vaccines remain key to combating COVID-19 morbidity and mortality, it is increasingly evident that VE varies by target population. While SARS-CoV-2 mRNA vaccines have demonstrated VE across a range of ages, they have been less effective at preventing hospitalization and symptomatic infection 9.5% reduction in VE in those >65 years (Y) versus 18-65Y adults,[1] and 20% less efficacy in >80Y compared to 60-69Y.[5] A meta-analysis identified a 9.3% decrease of VE preventing infection in older populations compared to the general populace,[6] and another review identified consistently lower VE in those ≥65 than <65, with up to 15% less VE in elders.[7] Generally, age-associated infection vulnerability has been attributed to increased disease severity and reduced vaccine-induced protection.[5,8–10] Vulnerability, linked with immunosenescence in older adults, has been observed both with respect to SARS-CoV-2 infection-induced immunogenicity[11] and reduced immunogenicity of mRNA vaccines.[12–18] These observations mirror impaired

[1]*Precision Vaccines Program*, Department of Pediatrics, Boston Children's Hospital, Boston, MA 02115, USA
[2]Department of Pediatrics, Harvard Medical School, Boston, MA 02115, USA
[3]Prevention of Organ Failure (PROOF) Centre of Excellence, St Paul's Hospital, University of British Columbia, Vancouver, BC V6Z 2K5, Canada
[4]UBC Centre for Heart Lung Innovation, Providence Research, St Paul's Hospital, Vancouver, BC V6Z 1Y6, Canada
[5]Department of Medicine, Division of Infectious Diseases, Brigham and Women's Hospital, Boston, MA 02115, USA
[6]Research Unit of Clinical Immunology and Vaccinology, Bambino Gesù Children's Hospital, IRCCS, 00165 Rome, Italy
[7]Department of Systems Medicine- Chair of Pediatrics, University of Rome, 00133 Tor Vergata, Italy
[8]Center for Pathogen Research, Department of Microbiology and Immunology, The University of Maryland School of Medicine, Baltimore, MD 21201, USA
[9]Global Investigative Toxicology, Preclinical Safety, Sanofi, Cambridge, MA 02142, USA
[10]Broad Institute of MIT & Harvard, Cambridge, MA 02142, USA
[11]Department of Pathology, Boston Children's Hospital, Harvard Medical School, Boston, MA 02115, USA
[12]These authors contributed equally
[13]Lead contact
*Correspondence: david.dowling@childrens.harvard.edu (D.J.D.), ofer.levy@childrens.harvard.edu (O.L.)
https://doi.org/10.1016/j.isci.2024.111055

immunogenicity in elder individuals across a range of vaccines targeting diverse microbial pathogens,[19–23] impacting both humoral and cell-mediated immunity, culminating in diminished VE in older adults.[13,24–26]

Reduced vaccine immunogenicity in older adults likely reflects immunosenescence. Advancing age has been associated with impaired immunity including reduced neutralization, phagocytosis, chemotaxis, and co-stimulatory molecule expression.[14,20,27] This impairs B cell class switching, with distinct T follicular helper $CD4^+$ T cell (T_{FH}) activity, and increased T regulatory cell (T_{reg}) frequency restraining responses.[14,19–23] Age-associated changes in T cell immunity could contribute to reduced cellular and antibody (Ab) functionality following the mRNA vaccination of older adults.[12,13,16] Older populations (>60Y, >65Y, and >80Y) demonstrate lower cell mediated immunity (CMI), with impaired $CD4^+$ and $CD8^+$ activation following BNT162b2 immunization, compared to middle aged adults.[14,15,28] Impaired $CD4^+$ and $CD8^+$ T cell responses were also observed in older adults post-SARS-CoV-2 infection,[29] suggesting distinct immunity. Additional booster immunizations with mRNA vaccines encoding Wuhan1 or bivalent Wuhan1 with BA.4/BA.5 mRNA encoding spike protein have been applied to overcome elder immunosenescence.[30–32] The third immunization with Wuhan1 mRNA transiently amplified immunogenicity against Wuhan1, and the variants Delta (B.1.617.2), and Omicron (B.1.1.529),[30] but failed to induce durable immunity as >65Y individuals had more rapid waning of immunity compared to <65Y.[31] The CDC Advisory Committee on Immunization Practices (ACIP) recommendation for those ≥65 Y to receive 2 mRNA immunizations per year was driven by expected and exacerbated waning immunity in elder populations.[33] A better understanding of age-specific immunity may provide insights that can inform efforts to optimize mRNA vaccines to enhance VE.

An emerging approach to characterize vaccine action is human *in vitro* modeling,[34] employing primary human leukocytes and autologous plasma, which is a rich source of age-specific soluble factors.[9,34–37] Indeed, the recent passage into law of the FDA Modernization Act 2.0 provides for the use of human *in vitro* systems to support drug and vaccine development.[37] Such *in vitro* systems enable the characterization of vaccine action in a species-specific manner wherein the same study participant can serve as the control (vehicle) and test condition. Such assays are amenable to the downstream measurement of a range of analytes via systems biology enabling the discovery of biomarkers that may correlate with vaccine safety (e.g., reactogenicity) and immunogenicity *in vivo*. Characterizing mRNA vaccine-induced immune activation *in vitro* may provide insight into human- and age-specific immunogenicity to inform future enhancement and optimization of mRNA vaccines.

We hypothesized that comparing responses of young and older adults to mRNA vaccines via human *in vitro* modeling coupled with proteomics would demonstrate distinct age-specific responses to BNT162b2 stimulation, providing an understanding of age-specific mRNA vaccine immune activation. To this end, we studied BNT162b2 immune stimulation in adult and elder human whole blood assay (WBA) *in vitro* and characterized the supernatant proteomes using liquid chromatography mass spectrometry (LC/MS), Ab-based proximity extension assay (PEA), as well as cytokine and chemokine multiplexing. We observed impaired induction of a range of proteins including T_H1-polarizing cytokines and chemokines in elders. This age-dependent mRNA vaccine-induced impaired T_H1 immunogenicity was confirmed in young and aged mice, *in vivo*. Impaired T_H1 polarization with age may contribute to the reduced mRNA vaccine-induced immunogenicity that is observed in older adults. These observations provide insight into age-dependent mRNA vaccine action and can inform the discovery and development of next generation vaccines optimized for enhanced immunogenicity and protection in vulnerable older adults with distinct immunity.

RESULTS

Cohort description

Human research study participants donated peripheral blood which was evaluated *in vitro* for immune activation following stimulation with the BNT162b2 lipid nanoparticle (LNP) encapsulated mRNA vaccine (*Pfizer/BioNTech*). Participants were grouped by age, with younger and middle-aged adults of 18-50Y, and older adults, elders, ≥ 60Y. These populations had a mixed vaccination and infection history, detailed in Tables S1 and S2. In brief, 41% of adults evaluated had a self-reported exposure to SARS-CoV-2 Spike antigen via infection or vaccination, while 86% of elder participants had a self-reported exposure.

BNT162b2-stimulation impacts the whole blood proteome

Human blood was stimulated with an mRNA LNP in a whole blood assay (WBA), broadly measuring up-/down-regulation and age-associated differences of immune factors by supernatant LC/MS proteomics (n = 12–14, Table S1). LC/MS has been employed to identify disease severity-associated responses after SARS-CoV-2 infection in humans,[38] but has not yet been employed to evaluate *in vitro* WBA with BNT162b2-stimulated supernatant. Protein expression was evaluated by generalized estimating equations generalized linear model (GEEGLM) analysis,[39–42] assessing mRNA vaccine stimulant concentration-dependent impact on analyte fold change (FC) of stimulated over matching vehicle control for baseline-normalization. Adult participants had 20 upregulated and 4 downregulated proteins (Figure 1A), while elder participants demonstrated 4 upregulated and 12 downregulated proteins (Figure 1B). Heatmap visualization displayed age-dependent patterns of the regulation (Figures S1A and S1B). Notable BNT162b2-induced proteins in adults included a proteasome regulatory unit protein (PSMC6), hemoglobin subunit epsilon (HBE1), carboxypeptidase N catalytic chain (CPN1), and bisphosphoglycerate mutase (BPGM). Downregulated proteins included peptidyl-prolyl *cis-trans* isomerase A (PPIA) and neutrophil defensin 3 (DEFA3). Elder sample protein upregulation included serum amyloid A-1 protein (SAA1) and the fibrinogens-γ and -β (FGG and FGB), while downregulated proteins included DEFA3, tropomyosin alpha-4 chain (TPM4), apolipoprotein F (APOF), apolipoprotein C-II (APOC2), CPN1, and peptidase inhibitor 16 (PI16). The supernatant was further evaluated with 4 Target 96 kits (inflammation, inflam; oncology III, onco; neurology, neuro; and cardiometabolic, cardio) of

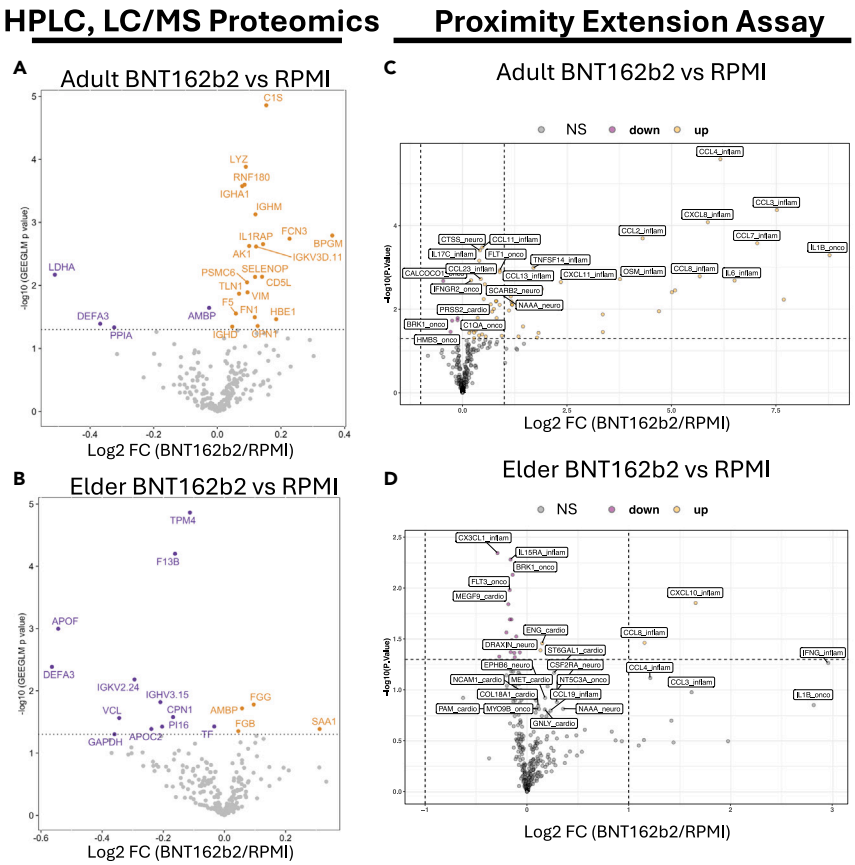

Figure 1. mRNA vaccine induced greater *in vitro* inflammatory protein release in adult vs. elder whole blood assay

Adult and elder whole blood stimulated with vehicle control (RPMI) or BNT162b2 had supernatants characterized by LC/MS (A-B) and PEA (C-D). GEEGLM evaluation testing concentration-dependent down- (purple) and up-regulated (orange) protein expression is presented against log_2FC of BNT162b2-stimulated samples over matching control, from (A) adult and (B) elder participant samples. Log_2FC of 2μg/ml BNT162b2's mRNA over matching vehicle control display PEA-quantified (C) adult and (D) elder responses. Horizontal dotted lines represent -log10(0.05). For (A-B) n = 10 to 14; for (C-D) n = 4 to 5. Statistical significance was determined by (A-B) GEEGLM, and (C-D) paired moderated T-test.

PEA-based proteomics, quantifying 368 proteins (from n = 4–5 participants, Table S2). PEA of supernatants identified the upregulation of predominantly inflammatory markers in adult BNT162b2-stimulated samples compared to vehicle (e.g., chemokine (C-C motif) ligand 2 (CCL2), CCL3, CCL4, CCL7, CCL8, CCL11, chemokine (C-X-C motif) ligand 8 (CXCL8), IL-1β, and IL-6),[38,43–49] with 60 upregulated and 5 downregulated differentially expressed proteins (DEPs) with nominal $p < 0.05$ (Figure 1C, 21 upregulated and 1 downregulated with Benjamini-Hochberg false discovery rate (FDR) < 0.05). In stark contrast, the only PEA-quantified inflammatory markers induced in BNT162b2-stimulated elder participant samples, compared to vehicle control, were CCL8 and CXCL10 (Figure 1D). In general, elder participant blood samples were less responsive to BNT162b2 stimulation, totaling 4 upregulated and 16 downregulated DEPs with $p < 0.05$ (0 DEP with FDR <0.05). Unsupervised heatmap evaluation of the top 30 DEPs resulted in 4/5 adult samples clustering by treatment versus no clustering in the elder study participants (Figures S1C and S1D).

The inflammatory proteome was lower in elders' than adults' BNT162b2-stimulated whole blood

BNT162b2-induced LC/MS proteomic protein profiles in the WBA differed by age, with adults and elders expressing 21 and 13 unique proteins, respectively (Figure 2A). Just 3 significant DEPs overlapped across age groups, with only DEFA3 downregulated in response to BNT162b2 stimulation in both age groups. The other 2 overlapping proteins had different directionality (Alpha-1 microglobulin, AMBP, was downregulated in adults but upregulated in elders, and vice versa for CPN1). BNT162b2 generally induced greater responses in adults vs. elders (Figures 2B, S2A and S2B). Principal component analysis (PCA) clustering of PEA proteomics displayed distinct adult and elder patterns with separation only in adult BNT162b2-stimulated vs. vehicle control (RPMI, Figure S2C). PEA comparison of BNT162b2-stimulated adult vs. BNT162b2-stimulated elder samples also demonstrated a generally greater upregulation of inflammatory markers in adults (Figure 2C). Advancing age had a significant correlation with lower BNT162b2-induced CCL4 (BNT162b2 stimulation slope −0.13, $p = 0.04$, Figure 2D), with trends toward lower CXCL8 (BNT162b2 stimulation slope −0.1, $p = 0.09$), and CCL2 expression (BNT162b2 stimulation

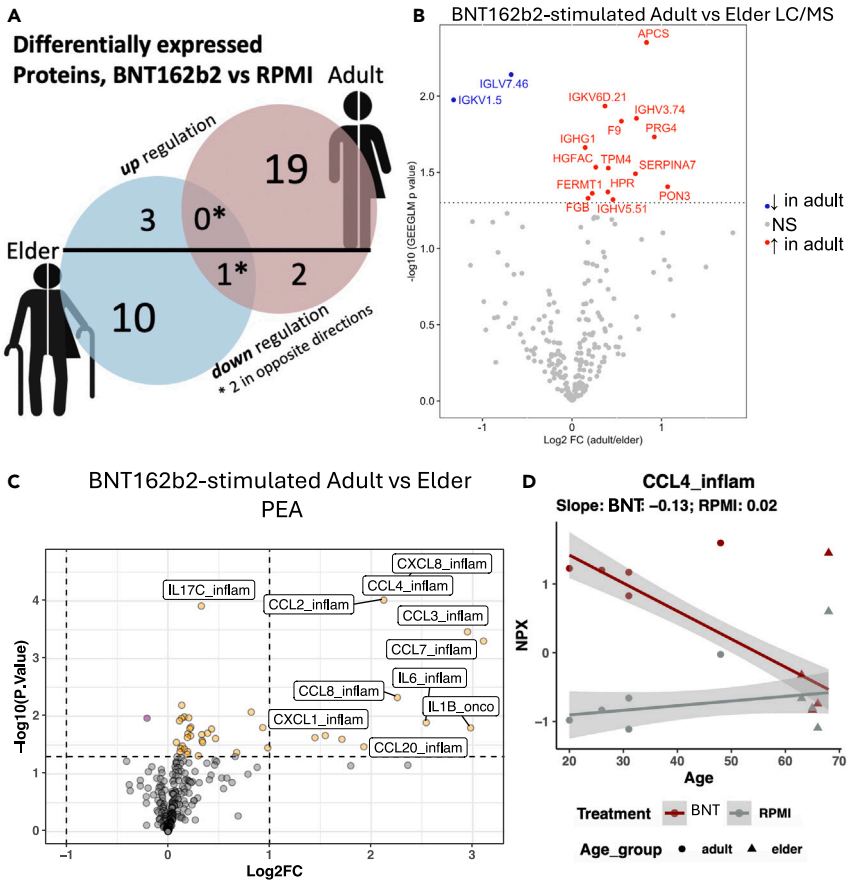

Figure 2. Lower BNT162b2-induced inflammatory response in elder vs. adult whole blood assayed *in vitro*

(A) DEPs from BNT162b2-stimulated samples against paired vehicle controls (RPMI) were predominantly nonoverlapping between age groups. Comparing BNT162b2-stimulated adult and elder samples identified upregulation in adult participants with analyte quantification by (B) LC/MS-proteomics or (C) PEA-proteomics. (D) Advancing age (years, Y) negatively correlated with normalized protein expression (NPX) in BNT162b2 (BNT)-induced CCL4 (Spearman's correlation analysis $p = 0.04$), with 95% confidence interval graphed in gray. (B-C) Horizontal dotted lines represent -log10(0.05). For (A-B) $n = 10$ to 14; for (C-D) $n = 4$ to 5. Statistical significance was determined by (B) GEEGLM, (C) paired moderated T-test, and (D) Spearman's correlation.

slope −0.07, $p = 0.11$) (Figure S2D). Network representation of DEP pathway analyses indicated some similar pathways induced in adult and elder participant samples (Figures S2E and S2F, E g., "signaling by interleukins"). Elder sample profiles had fewer proteins contributing to each pathway node and an additional predominantly downregulated "immunoregulatory interactions between a lymphoid and a non-lymphoid cell" node that was not observed in adult study participants. Additionally, the "IL-4 and IL-13 signaling" that was enriched in adult samples was not observed in elder samples. Overall, BNT162b2 mRNA vaccine stimulation in the WBA resulted in dampened proteome responses in elder participant samples across two proteomic platforms.

Cytokine and chemokine induction by BNT162b2 was verified by bead-based multiplex, with lower T_H1 support from aged participants

An additional evaluation by a targeted multiplex bead-based assay identified titratable production of interleukin-6 (IL-6), CXCL8, tumor necrosis factor (TNF), and interferon gamma (IFNγ) in adult WBA samples (Figure 3A). Other cytokines measured, such as IL-17A, were not induced. Adult and elder responses were FC-normalized (stimulated divided by paired vehicle control) (Figure 3B), and multiple analytes were induced in both age groups, including CXCL10, IL-1RA, and IFNγ. Nevertheless, across multiple stimulation doses, elder samples had 30-59% lower IFNγ, 42–85% lower CXCL10, and 54–85% lower IL-1RA FC induction, compared to adults. Importantly, CXCL10, IFNγ, IL-1RA, and CCL4 have been associated with high responsivity in young adults following human mRNA vaccine immunization,[50] that was also higher in adults than in elders (Figure 3C). Multiplex-quantified analytes were grouped by function (per Table S3) as T_H1, T_H2, T_H17, or T regulatory (T_{reg}) polarizing, chemokine, hematopoiesis-supporting, or those associated with trained immunity. A linear modeling analysis, GEEGLM, evaluated if age interacted with each function. T_H1 support was significantly impaired ($p = 0.027$) in elders compared to adults,

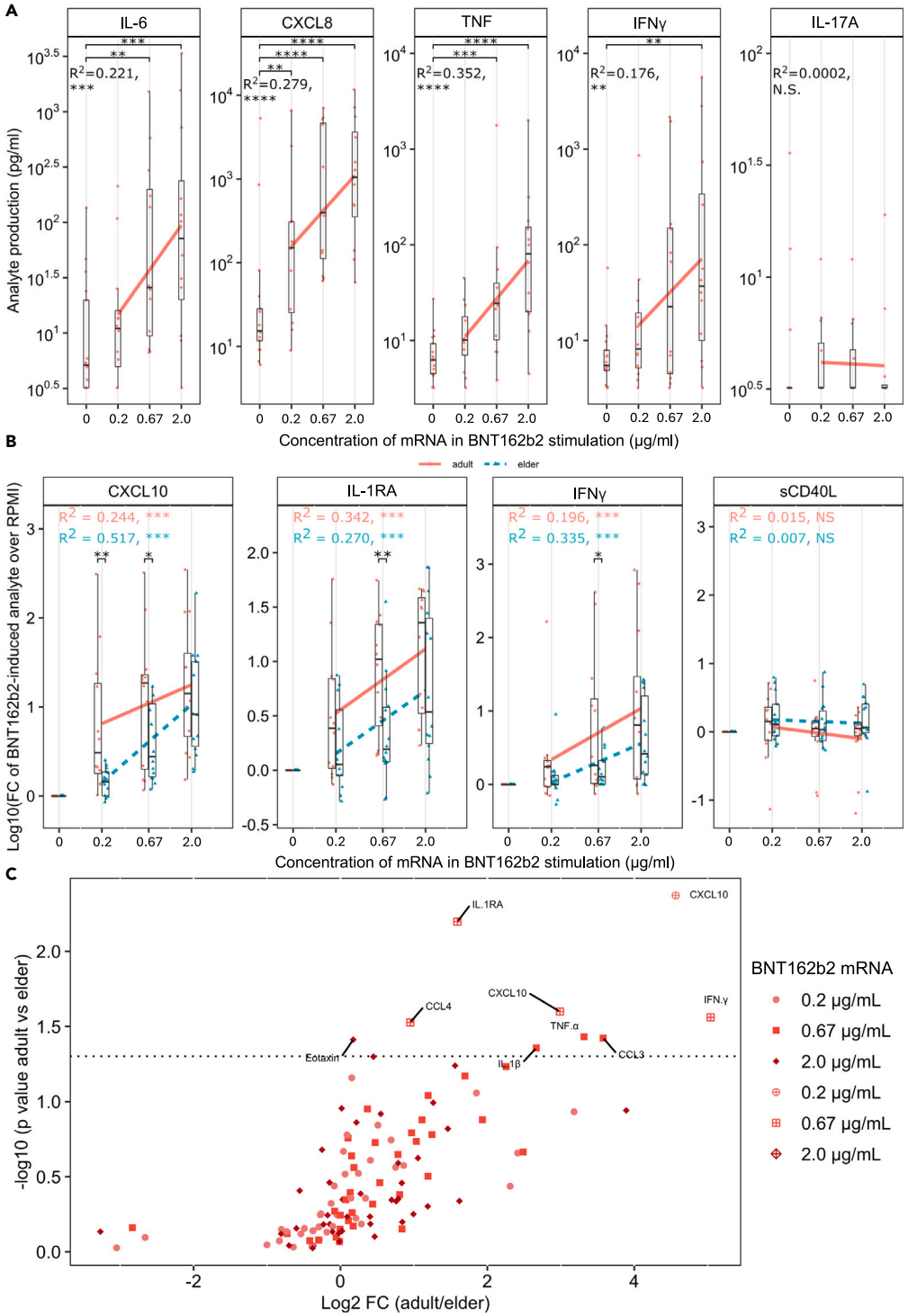

Figure 3. BNT162b2 induced concentration- and age-dependent cytokine and chemokine production in *in vitro* human whole blood assay

Multiplex quantification of secreted analytes identified BNT162b2-induced responses compared to vehicle control (RPMI).

(A) mRNA vaccine concentration-dependent induction of IL-6, CXCL8, TNF, and IFNγ was noted in adults.

(B) Fold Change (FC) baseline standardization of stimulated over matching vehicle control demonstrated greater production of certain analytes such as CXCL10, IL-1RA, and IFNγ in adult (solid red line) vs. elder (dashed blue line) blood.

(C) Volcano plot of analytes with greater BNT162b2 fold-induced stimulation in adults than in elders, with circles representing 0.2 µg/mL, squares 0.67 µg/mL, and diamonds 2.0 µg/mL of mRNA encapsulated in BNT162b2. Non-filled, crossed points represent markers associated with high vaccine responsiveness. The dotted

Figure 3. *Continued*

line represents significance, with points annotated above 1.3 -log10(*p*-value). For (A-C) *n* = 12 to 14. Boxplots display the median, interquartile range (IQR), with the identification of the furthest values from the median not exceeding 1.5 × IQR. Statistical significance was determined by Shapiro-Wilk then (A) paired Wilcoxon rank-sum test, (B, C) 1-sided unpaired T tests on log-transformed fold-change, with *p*-values annotated as *$p < 0.05$, **$p < 0.01$, ***$p < 0.001$, ****$p < 0.0001$.

with an average of 7.2% less in each analyte involved (Figures 4A–4C). The other functions evaluated were not significantly different (Figure S3) indicating a predominant impairment in inducing T_H1-polarizing analytes.

Reduced mRNA vaccine-induced T_H1 cellular immunity in aged compared to young adult mice

To assess whether the age-dependent differences observed *in vitro* may also be reflected *in vivo*, we assessed murine intramuscular BNT162b2 vaccination (Figure S4A). As observed in humans,[12,13] aged mice (>10 months) sera displayed significantly lower total immunoglobulin G (IgG), IgG2a, and IgG1 Ab immunogenicity, with a lower anti-receptor binding domain (RBD) Ab titers than adult mice (Figure 5A). Aged murine immunity was rescued with higher antigen doses, with non-significant differences between 0.5 μg-immunized adult and 1.0 μg-immunized elder, or 1.0 μg and 5.0 μg immunized adult and elder animals, respectively. Adult and aged mice displayed waning immunity between Days (D) 42 and 210 post-prime immunization, at various immunization doses (Figures S4B–S4G). Mirroring human elder observations,[31] greater waning of immunity was observed in 1 μg-immunized aged mice, with 63–75% more waning immunity across IgG, IgG2a, and IgG1 based on the median fold change of D210 over D42 between age groups (Figure S4H). A trend of 30–83% faster waning was observed at other immunization doses. Ab isotypes IgG2a and IgG1, respective markers of T_H1 and T_H2 polarized immunity,[51] were induced over non-vaccinated controls (Figure 5A). The IgG2a/IgG1 relative ratio inferring T_H1 (>1) or T_H2 (<1) polarization identified an impairment of T_H1 associated responses in aged mice on D28 post-prime (dual immunized), but not D14 post-prime (singly immunized) (Figures S5A and S5B). Ab function was inferred via sera inhibition of RBD binding to recombinant human angiotensin-converting enzyme 2 (hACE2) in a surrogate virus neutralization assay (sVNT), as a correlate of protection.[52,53] Aged mice had lower sVNT than adult mice at multiple immunization doses (Figure S5C). A Spearman's rank correlation test was performed in both age groups, measuring whether an independent variable, anti-spike protein IgG Ab response, statistically significantly correlates with a dependent variable, sVNT. Spearman's rho correlation coefficients, measuring the strength (+1 or −1 rho representing perfect associations, and 0, no association) and direction (a positive rho indicating that increasing one variable would increase the other) of the correlation between anti-spike IgG and sVNT, were r = 0.87 and r = 0.75 for adult and aged mouse groups, respectively (Figure S5D). D28 post-prime murine Ab neutralization of live Washington-1 (WA-1) SARS-CoV-2 *in vitro* demonstrated an impaired aged response compared to adult mice (Figure S5E). Spike peptide splenocyte stimulation induced $CD4^+$ T cell IFNγ, IL-2, TNF, and dual stained IL-4 and -5 positivity, alongside $CD8^+$ TNF (Figure S6, key resources table). Baseline population differences in $CD4^+$ T cell populations were accounted for by dividing mouse BNT162b2-immunized responses by the average of age-matched vehicle control immunized mice. Aged mice had significantly less fold-induction of $CD4^+$ T cell IFNγ and TNF cell positivity compared to adult mice (59% and 43% lower median fold induction, respectively, Figure 5B). IL-2 was unchanged, while IL-4/5 demonstrated a lower trend in aged mice (54% lower median aged FC induction) that was not statistically significant. Similarly, $CD8^+$ TNF^+ T cell fold induction was significantly impaired in aged vs. adult mice (45% less median elder FC, Figure 5C). Overall, *in vivo* murine evaluation mirrored human results with age-associated impaired Ab production, Ab function, class switching, and $CD4^+$ and $CD8^+$ CMI.

DISCUSSION

Herein, we have characterized BNT162b2-induced immunity with the proteomic assessment of age-specific human whole blood stimulation *in vitro*. We demonstrate that (a) human *in vitro* modeling of proteomic responses to mRNA vaccines is feasible, (b) such modeling demonstrates marked age-dependent differences in mRNA vaccine-induced analytes including those supportive of T_H1 immunity; (c) impairment in mRNA vaccine-induced T_H1 polarized responses was validated in mice, and (d) analytes identified *in vitro* (e.g., IFN-γ, CXCL10, IL.1RA, CCL4) corresponded with those that correlated with higher immunogenicity in humans, *in vivo*, following mRNA vaccination. Vaccines have been crucial in combatting the SARS-CoV-2 pandemic and mRNA vaccines are being assessed for utility against other infectious and non-infectious diseases, yet much remains to be learned regarding their age-specific immunogenicity.[13,24–26,54] As elders have higher rates of severe COVID-19[55] and reduced vaccine immunogenicity,[12–15,28,56] understanding the contributing factors to weaker immunogenicity is an urgent unmet need.

While the mechanisms of mRNA vaccine activation are under active investigation, a possible contribution from self-adjuvantation from ionizable lipids and mRNA can enhance immunogenicity.[57–60] Self-adjuvantation has been associated with high efficacy in live-attenuated vaccines, arising from pathogen-associated molecular patterns activating and enhancing innate immune responses.[61–63] Immune activation following BNT162b2 stimulation may be mediated by pattern recognition receptors (PRRs) such as Toll-like receptor (TLR)-2, −3, −4, −7, and/or −8, as well as retinoic acid-inducible gene I (RIG-I), and melanoma differentiation-associated protein 5 (MDA-5) recognizing multiple vaccine components.[64–67] Among other PRRs, SARS-CoV-2 can also activate MDA-5 signaling.[68] Development of vaccine formulations that trigger similar innate immune activation as natural infection may enhance immunogenicity against microbial pathogens.[62,69] Consequently, DEPs from BNT162b2 stimulation were compared to SARS-CoV-2 infection-associated responses. We employed two complementary proteomic approaches for the *in vitro* evaluation of BNT162b2-induced WBA responses. LC/MS proteomics identified DEPs of BNT162b2-stimulated WBA adult samples compared to vehicle control (Figure 1). Adult samples, but not those from older adults, demonstrated

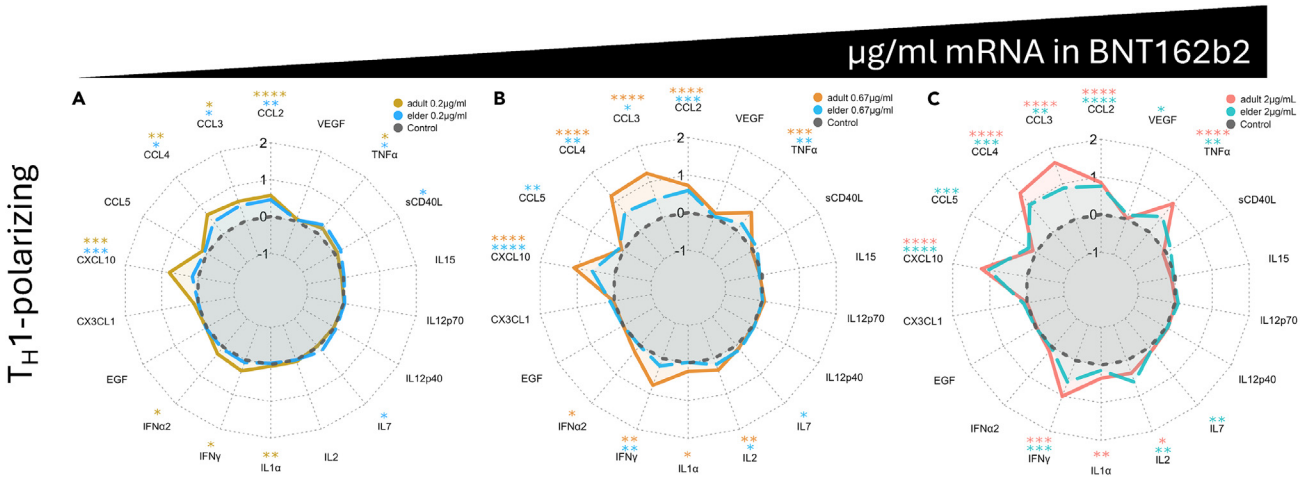

Figure 4. Impaired BNT162b2-induced T_H1-polarizing cytokine production in human older vs. young adults' blood

Radar plots displaying log_{10}-transformed, FC averages of multiplex-quantified analytes per spoke, separating adult (orange-red) and elder (blue-teal) participants. Stimulation with BNT162b2 (BNT) encapsulated mRNA weights of (A) 0.2 µg/mL, (B) 0.67 µg/mL, and (C) 2 µg/mL had T_H1-polarizing analytes (per Table S3) significantly induced (one-sided T-tests hypothesizing induction compared to vehicle control, color-coded orange adult and teal elder asterisks presented above each analyte). GEEGLM analyses evaluating the interaction of age and induction of T_H1 polarizing analytes demonstrated 7.2% less T_H1-polarizing cytokine production in elder participant samples compared to adult samples ($p = 0.027$). For (A-C), $n = 12$ to 14. Significance displays one-sided unpaired T-tests compared to vehicle control, with p-values annotated as $*p < 0.05$, $**p < 0.01$, $***p < 0.001$, $****p < 0.0001$.

BNT162b2-induced increases in the ATPase PSMC6, hemoglobin HBE1, and the metalloprotease CPN1, each implicated in the host response to SARS-CoV-2, COVID-19 severity, and/or have anti-viral activity.[70–75] Additionally, stimulated adult, but not elder, samples had reduced peptidylprolyl isomerase A (PPIA), lower plasma concentrations of which are associated with better COVID-19 prognosis.[76]

Elder participants' proteomic responses were markedly distinct from adults. There was only a single overlapping downregulated protein between the age groups assessed by LC/MS, DEFA3 (Figure 1), which has been associated with lipid envelopes.[77] Adult participants had 19 up- and 2 down-regulated proteins, while elder participants had a starkly contrasting 3 up- and 10 down-regulated proteins, highlighting divergent immune responses (Figure 2A). Unique proteins included SAA1, FGG, and FGB which were induced in elder BNT162b2-stimulated samples, but not adults, and have been associated with SARS-CoV-2 infection and/or COVID severity.[78–81] Downregulated DEPs in BNT162b2-stimulated elder samples, compared to vehicle control stimulations, included TPM4, APOF, APOC2, CPN1, and PI16, which were also downregulated by exposure to SARS-CoV-2 virions in humans *in vitro* and *in vivo*, associating with poor prognosis.[75,82–84] Overlap of impaired elder BNT162b2 responses with factors that have been associated with disease susceptibility may reflect important common signaling pathways shaped by immunosenescence that may contribute to both COVID susceptibility and impaired vaccine responses. A secondary guided PEA-based proteomic assay validated results (Figures 1C and 1D), observing similar age-dependent patterns of BNT162b2-induced adult up and elder downregulation as the LC/MS proteomics, but with distinct analytes. The striking differences in proteomic responses between adult and elder participants may contribute to age-dependent differences in BNT162b2 immunogenicity.

Directly comparing the proteome derived from BNT162b2-stimulated adult and elder WBA supernatants via LC/MS (Figure 2B) and PEA (Figure 2C) demonstrated marked age-dependent differences. Antibody and bead-based fluorescent multiplex analysis revealed that elders had significantly ($p = 0.04$) impaired BNT162b2-stimulated chemokine CCL4 production (Figure 2D), though the functional categorization of multiplex-quantified chemokines did not identify broad differences in chemokine induction (Figure S3). CCL4 induction has been negatively correlated with age,[20] potentially impacting monocyte and antigen-presenting cell (APC) chemotaxis to the injection site and lymph nodes, respectively,[85–88] both of which would impact adaptive immunity. Network analysis of DEPs (Figures S2E and S2F) further delineated lower mRNA vaccine-induced activation in elderly blood. In contrast to young adults, elder participant samples lacked BNT162b2-induced activation of the '*IL-4 and IL-13 signaling*' network which supports T_H2, B cell differentiation, and class switching.[89] Additionally, while adults had an unaltered pathway, elders demonstrated BNT162b2-induced down-regulation of the "*immunoregulatory interactions between a lymphoid and non-lymphoid cell*" pathway. An associated analyte within this pathway, Cytotoxic and regulatory T cell molecule (*CRTAM*), supports $CD4^+$ and $CD8^+$ T cell differentiation,[90] such that downregulation in elders may contribute to reduced CMI.

BNT162b2 stimulation in a whole blood assay (WBA) resulted in dose-dependent induction of multiple analytes, including IL-6, CXCL8, TNF, and IFNγ (Figure 3A). The WBA induced similar analytes as those from adult human *in vitro* stimulations with LNP encapsulated mRNA (encoding non-SARS-CoV-2 antigens and with a distinct cationic lipid, SM-102),[91] IL-1β, IL-1RA, IL-6, TNF, CCL2, CCL3, and CCL4 (Figures 4 and S3), indicating similar immune activation of peripheral lymphocytes in a WBA. Myocarditis, a serious mRNA vaccine-associated adverse event, has been correlated with vaccine-induced plasma IL-1β, IL-1RA, IL-15, CCL4, CXCL1, and CXCL10,[92] each of which was also significantly induced *in vitro* with WBA BNT162b2 stimulation (Figures 4 and S3), demonstrating the potential utility of the WBA platform

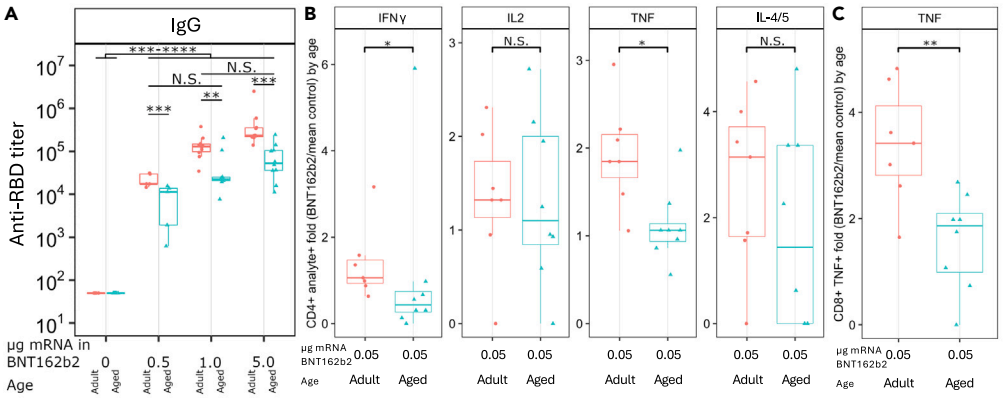

Figure 5. Reduced humoral and T_H1 cellular immunogenicity of BNT162b2 vaccine in aged mice

BNT162b2-immunized adult and aged mice had humoral immunity evaluated on Day 42 post-prime immunization for receptor binding domain (RBD) responsivity. (A) Total anti-RBD IgG was significantly induced, but with significantly lower Ab titers in aged mice. With FC normalization, aged mice additionally had (B) lower $CD4^+$ T cell $IFN\gamma^+$ and TNF^+ (T_H1) positivity, and (C) lower $CD8^+$ T cell TNF^+ positivity. For (A-C), n = 5 to 10. Boxplots display the median, interquartile range (IQR), with the identification of the furthest values from the median not exceeding 1.5 × IQR. Statistical significance was determined by Shapiro-Wilk, then (A) Kruskal-Wallis and one-sided Wilcoxon rank-sum hypothesizing vaccine-associated induction compared to vehicle control, and two-sided Wilcoxon rank-sum test comparing age groups, (B) two-sided Wilcoxon rank-sum, (C) two-sided T-test, with significance annotated as *$p < 0.05$, **$p < 0.01$, ***$p < 0.001$, ****$p < 0.0001$.

for studying vaccine safety. Lower mRNA vaccine-induced reactogenicity in older adults has been associated with lower immunogenicity,[93] therefore mRNA vaccine activation of the innate immune system may concurrently contribute to both mRNA vaccine self-adjuvantation and reactogenicity.

BNT162b2-induced WBA cytokine and chemokine induction were age-dependent with consistently observed lower elder participant responsivity across LC/MS proteomics, PEA proteomics, and multiplex platforms. Functionally, T_H1-polarized immunity is observed after BNT162b2 and mRNA-1273 immunization,[94–96] but is not equally induced across multiple age groups. Human elders have impaired induction of antibody isotypes IgG1 and IgG3,[97] associated markers of human T_H1 polarization,[98,99] and also have had direct impairment of $CD4^+$ and T_H1 polarized T cell responses following BNT162b2-immunization.[15,100] Specific contributing mechanisms to age associated BNT162b2 responsivity have not yet been described. Post-BNT162b2 mRNA vaccination, systemic IL-1RA, and the T_H1-polarizing CXCL10, CCL4, and IFNγ[101–108] production have been associated with higher SARS-CoV-2 specific immunogenicity in 28–59-year-old adults.[50] Of note, older adults demonstrated lower production of IL-1RA, CXCL10, CCL4, and IFNγ *in vitro* (Figures 3B and 3C), analytes associated with higher human immunogenicity *in vivo*.[50] These analytes may be pivotal as the T_H1 polarizing cytokine IFNγ can suppress T_H2-associated IL-4, and increase expression of IL-12p70 and its receptor.[107] Indeed, blocking IFNγ has been shown to impair BNT162b2 responsivity in adult mice.[109] These observations are consistent with the impaired production of IFNγ by monocyte derived Dendritic Cells (MoDCs) from older vs. young adults to other lipid nanoparticles.[110] Reduced production of CXCL10 by older adults may constrain vaccine immunogenicity as exogenous CXCL10 incubation with naive T cells can support T_H1 and T_H17 cell differentiation,[104] DC-produced CXCL10 can promote lymph node DC-T-cell interactions during naive cell priming,[111] and knockout mice have impaired antigen-specific T cell responses.[108]

Interpretation of polyfunctional cytokines was validated by functionally grouping analytes to measure broadly dysregulated T_H1, T_H2, T_H17, or T_{reg} polarizing, chemokine, hematopoiesis-supporting, or trained immunity-associated responses. Pairing individual analysis with functionally grouped analytes (Table S3) can broadly describe function-based differences to account for analyte redundancies.[112] Importantly, the functional assignment was not just based on being produced by a polarized cell but rather required evidence of supporting or being a polarizing molecule of naive T cells. A conservative GEEGLM analysis was employed, averaging the induction of functionally grouped analytes, including those that were not individually induced, thereby biasing toward no difference, so that only broad and significant differences would be observed. GEEGLM analysis identified a significant reduction (average 7.2% across analytes, $p = 0.027$) of T_H1 polarizing analyte induction in elder WBA responses (Figure 4). The other 6 functions evaluated were not significant, indicating no impairment, or sample size limitations. Age impacts DCs, monocytes, natural killer, and T cells,[113–115] and additional investigation is needed to identify which specific cell types have age-impaired mRNA vaccine responses. We observed decreased production of multiple analytes, particularly a decrease in those polarizing toward T_H1, in human elder samples, compared to adult samples. Immunophenotyping the cellular origin of mRNA vaccine-induced cytokine production is an important consideration and warrants further investigation.

Investigating BNT162b2-induced immune activation *in vitro* offers significant insights into species (i.e., human)- and age-specific responses, but may not completely reflect relevant vaccine responses *in vivo*. To assess for correlates of our *in vitro* observations *in vivo*, we employed an age-specific murine mRNA vaccination model.[116–118] Increased age is associated with impaired human humoral immunity following BNT162b2 or mRNA-1273 vaccination.[1,13,31,119] Similar to humans, aged mice demonstrated impaired Ab induction at all immunization doses (Figure 5A), and waning immunity was more rapid in aged mice (Figure S4).[31,120] Higher antigen doses resulted in enhanced

immunogenicity in aged animals, restoring humoral titers and sVNT to levels observed in younger animals (Figures 5A and S5). Higher antigen doses for older adults have been recommended to be evaluated for mRNA SARS-CoV-2 vaccines,[13] and which may be tolerated given generally lower elder reactogenicity.[93] T_H1/T_H2 polarization was indirectly inferred by a relative ratio of IgG2a and IgG1 Ab isotypes, respective T_H1 and T_H2 BALB/c markers.[51] IgG2a/IgG1 after first immunization was moderately T_H2-shifted and not different between both age groups, while the post-booster was T_H1-shifted in adult, but not aged, mice (Figure S5), potentially indicating booster-specific impairments that may impact future vaccination campaigns. Immune polarization changes over time, with a shift toward IgG4 responses after repeated immunizations in humans, suggesting a shift toward the associated marker of anti-inflammatory and T_H2 polarization.[121,122] Sera neutralization capacity, an important correlate of protection,[52,53,123,124] was impaired in both sVNT and live-virus WA-1 SARS-CoV-2 assays in aged mice (Figure S5). The murine setting enabled a controlled environment, minimizing confounders, and mirrored age-dependent human observations of neutralization.[125] By Spearman's rank correlation, anti-spike IgG significantly correlated with sVNT immunity in both age groups (Figure S5). T cell support is essential to effectively develop humoral immunity and cytotoxic immunity against infected cells. T_H1-polarizing analytes and Ab isotypes infer polarization states, and direct T cell evaluation can provide additional insight. Stimulation of murine splenocytes with spike-specific peptide induced IFNγ and TNF in $CD4^+$ T cells, indicating T_H1 polarization,[126] with 43–59% less median induction of cell positivity in aged vs. young adult mice (Figure 5B). Additionally, aged mice had significant impairments in BNT162b2-induced TNF^+ $CD8^+$ T cells (Figure 5C), an important cell subset for lysing infected cells.[126] Reduced BNT162b2 immunogenicity in aged mice included lower vaccine-induced Ab titers, impaired Ab neutralization capacity, diminished $CD8^+$ T cell activity, and reduced T_H1 polarization of $CD4^+$ T cells, coupled with more rapid waning immunity, indicating the utility of murine models to investigate age-associated changes in immunity.

The observed impaired BNT162b2-induced T_H1 immunogenicity in aged mice and older human adults reflects distinct immunity with age. Multiple approaches may amplify immunogenicity, including: (a) dose-escalation,[13] (b) additional boosters to extend protection,[123,127] albeit temporarily, due to rapidly waning immunity in elders,[31] and (c) use of T_H1-polarizing adjuvants targeted toward elder populations,[9] including Alum:CpG, saponin, or MF59,[62,128–131] and potentially the TLR7/8 agonist Alhydroxiquim-II,[132] to enhance host defense against intracellular pathogens,[133,134] B cell class switching (human IgG1 and IgG3,[98,99] or murine IgG2a[98]), and support T_{FH}-independent B cell responses.[135]

Our study features multiple strengths, including (a) the use of a human WBA *in vitro* that is replete with age-specific cellular and soluble factors that preserve physiological states, and which may be predictive of vaccine responses *in vivo*,[35,136] (b) the use of three complementary proteomic approaches (mass spectrometry, PEA and multiplex assay) to gain a comprehensive view of the impact of BNT162b2 on the WBA proteome, and (c) validation of findings using aged vs. adult mice *in vivo*. The use of human *in vitro* assays enables human- and age-specific modeling with individuals serving as both control and test conditions, permitting paired analyses of new and established/licensed vaccine formulations, thereby accelerating and de-risking vaccine discovery and development.[34–36] Indeed, the U.S. FDA Modernization Act 2.0, signed into law in 2022, provides for the use of human *in vitro* systems coupled with bioinformatic biomarker analysis to advance drug and vaccine development.[37]

In summary, supernatants from adult and elder WBA demonstrated distinct BNT162b2-induced immune activation patterns by LC/MS and PEA proteomics, with BNT162b2-induced adult upregulation and elder downregulation. LC/MS DEP profiles were markedly age-dependent, with only 1 overlapping significant protein downregulated in both adults and elders (DEFA3). Cytokine and chemokine multiplex demonstrated a vaccine concentration-dependent response in human adults *in vitro*, including IL-6, CXCL8, TNF, and IFNγ production. Functional categorization of analytes identified impaired T_H1-polarizing analyte induction in elder participants, potentially contributing to reduced immunogenicity. Murine *in vivo* experiments mirrored impaired humoral induction, T_H1 polarization, reduced IgG2a/IgG1 relative ratio, and a directly reduced $CD4^+$ T cell IFNγ and TNF response to SARS-CoV-2 spike peptide. Our study has demonstrated the value of a human *in vitro* platform coupled with proteomic systems biology to model age-specific responses to the mRNA vaccine BNT162b2. As the U.S. FDA increasingly welcomes human *in vitro* data,[37] this approach may have broad applicability to advance mRNA vaccines that remain essential for combatting coronaviruses and hold great promise for protection against additional infectious diseases (e.g., influenza, RSV, and HIV), and in oncology.[57,137] Identifying age-specific responses to mRNA vaccines will inform the discovery and development of the next generation of precision mRNA vaccines to overcome immunosenescence. Given the potentially massive benefits of optimized vaccines,[138] further translational research is needed to enhance elder immune responses including expanded adjuvantation efforts to enhance T_H1 polarization, durable immunogenicity, and protection,[9] including through the addition of mRNA encoding IL-12 to adjuvant mRNA vaccines.[139,140]

Limitations of the study

As with any research effort, our study has multiple limitations, including (a) grouping into adult (18-50Y) and elder (≥60Y) categories (as in[141–145]) precludes other sub-age groups (e.g., 50-60Y, >80Y,[13,144] or >100Y[146]), (b) vaccine and infection history were self-reported and differential between groups, (c) the study is underpowered for small effects and therefore some observations of no significant difference may be Type II errors-i.e., failure to detect real differences, d) sample size precluded the assessment of confounders (e.g., obesity, corticosteroids, immunosuppression, cardiovascular disease, and smoking), and covariates (e.g., sex, gender, previous vaccination or infection, and so forth), requiring further investigation, (e) the *in vitro* WBA assay lacks fluid flow and tissue interaction (e.g., muscle), and did not identify cellular origin of T_H1 polarizing cytokine and chemokines, (potentially monocyte, macrophage, dendritic cells[109]), (f) study participants were not representative of global populations, (g) immune proteins have redundancies[112] lost during immunosenescence,[147] and (h) age-specific investigation of mice may not be directly translatable to humans.

RESOURCE AVAILABILITY

Lead contact

Request for further information, resources, and reagents can be directed to the lead contact, Dr. Ofer Levy (ofer.levy@childrens.harvard.edu).

Materials availability

This study did not generate novel reagents.

Data and code availability

- Deidentified quality assured human data from this study is deposited in the repository ImmPort:SDY2630, as listed in the key resources table. Further inquiries could be directed to the corresponding author. Murine data will be made available upon requests submitted to the corresponding author.
- This article does not report the original code.
- For other items, please contact the corresponding author.

ACKNOWLEDGMENTS

We thank the BCH Pharmacy and all our study participants, including members of the congregation of *Eitz Chayim* Synagogue (Cambridge, MA). We thank Dr. Benoit Fatou for assistance with proteomic sample processing and data analysis, Dr. Kinga Smolen for helpful discussions, as well as Drs. Sirano Dhe-Paganon and Hyuk-Soo Seo for the production of the recombinant spike and RBD antigens used in this study. We thank B. S. Graham (NIH Vaccine Research Center) for providing the plasmid for prefusion stabilized SARS-CoV-2 spike trimer. Katherine Chew, Maria DeLeon, Gandolina Melhem, and Yamile Lugo Rodriguez provided helpful technical support. We thank Dr. Emilie Clement, and Dr. Daniel Frederick of *Olink* for logistical and technical support. We thank the pharmacists of Boston Children's Hospital for efforts to maximize the use of SARS-CoV-2 vaccines by saving leftover (overfill) of otherwise-to-be-discarded vaccine vials, and Meagan Karoly and Caitlin Syphurs of the *Precision Vaccines Program* Data Management & Analysis Core for data deposition support. We thank Dr. Asimenia Angelidou and Project Manager Kerry McEnaney for supporting phlebotomy efforts. E.N. is a JSPS Overseas Research Fellow and a joint Society for Pediatric Research and Japanese Pediatric Society Scholar. We thank Dr. Natalie Thornburg and the CDC for providing WA-1 SARS-CoV-2. D.J.D. thanks S. McHugh, G. Boyer, L. Conetta and the staff of Lucy's Daycare, the staff the YMCA of Greater Boston, Bridging Independent Living Together (BILT) Inc., and the Boston Public Schools for childcare and educational support during the COVID-19 pandemic.

AUTHOR CONTRIBUTIONS

B.B. conceived, designed, performed, and analyzed the *in vitro* and *in vivo* experiments, and wrote the article. B.F. performed and analyzed LC/MS proteomics experiments. A.K.C. and J.A. analyzed PEA proteomics experiments. S.B. conceived, designed, performed, and analyzed flow cytometry experiments. C.S., A.N.B., and T.R.O. assisted with murine data acquisition. M.E.M., M.F. designed and performed true neutralization experiments. A.O., J.A., and H.S. advised analytical approaches. A.S., L.B., E.M., G.S.S., P.P., E.N., D.S., S.H., and H.S. contributed to experimental design discussions. All authors critically reviewed the article. D.J.D. and O.L. conceived the project, assisted with the design of the experiments, mentored B.B., and edited the article.

DECLARATION OF INTERESTS

O.L. has served as a consultant to GlaxoSmithKline (GSK) and Hillevax. M.B.F. serves on the scientific advisory board of Aikido Pharma and has collaborative research agreements with Novavax, AstraZeneca, Regeneron, and Irazu Bio. B.B., E.N., T.R.O., D.S., S.H., O.L., and D.J.D. are named inventors on vaccine adjuvant patent(s). O.L., G.S.S., and D.J.D. are named inventors on patents related to human *in vitro* modeling of vaccine responses. O.L. and G.S.S. are recipients of a sponsored research agreement with GSK. D.J.D is on the scientific advisory board of EdJen BioTech and serves as a consultant with Merck Research Laboratories/Merck Sharp & Dohme Corp. (a subsidiary of Merck & Co., Inc.). O.L. and D.J.D. are co-founders of and advisors to *Ovax, Inc.* ACS and LRB are involved in HIV, COVID, and other vaccine clinical trials conducted in collaboration with the NIH, HIV Vaccine Trials Network (HVTN), COVID Vaccine Prevention Network (CoVPN), International AIDS Vaccine Initiative (IAVI), Crucell/Janssen, Moderna, and Sanofi. These commercial or financial relationships are unrelated to the current study.

The participating *Precision Vaccines Program* (PVP) laboratories were supported in part, by U.S. National Institutes of Health (NIH)/National Institutes of Allergy and Infectious Diseases (NIAID) awards, including Human Immunology Project Consortium award U19 AI118608, Adjuvant Discovery (HHSN272201400052C) and Development (HHSN272201800047C) Program Contracts to O.L.; Adjuvant Discovery Program contract (75N93019C00044) to O.L. and D.J.D as well as NIH grant (1R21AI137932-01A1) to D.J.D. O.L. is also funded by an award from the Coalition for Epidemic Preparedness Innovations (CEPI), via the International Network of Special Immunization Services (INSIS). The PVP is supported, in part, by the BCH Department of Pediatrics and philanthropy via the BCH Trust, including from the Barry Family and the Boston Investment Council. A.K.C. was supported by the Friedman Award for Scholars in Health, the University of British Columbia, and Mitacs Accelerate Canada.

STAR★METHODS

Detailed methods are provided in the online version of this paper and include the following:

SUPPLEMENTAL INFORMATION

Supplemental information can be found online at https://doi.org/10.1016/j.isci.2024.111055.

Received: September 5, 2023
Revised: July 5, 2024
Accepted: September 24, 2024
Published: September 26, 2024

REFERENCES

1. Baden, L.R., El Sahly, H.M., Essink, B., Kotloff, K., Frey, S., Novak, R., Diemert, D., Spector, S.A., Rouphael, N., Creech, C.B., et al. (2021). Efficacy and Safety of the mRNA-1273 SARS-CoV-2 Vaccine. N. Engl. J. Med. *384*, 403–416. https://doi.org/10.1056/NEJMoa2035389.
2. Polack, F.P., Thomas, S.J., Kitchin, N., Absalon, J., Gurtman, A., Lockhart, S., Perez, J.L., Pérez Marc, G., Moreira, E.D., Zerbini, C., et al. (2020). Safety and Efficacy of the BNT162b2 mRNA Covid-19 Vaccine. N. Engl. J. Med. *383*, 2603–2615. https://doi.org/10.1056/NEJMoa2034577.
3. Dhakal, S., and Klein, S.L. (2019). Host Factors Impact Vaccine Efficacy: Implications for Seasonal and Universal Influenza Vaccine Programs. J. Virol. *93*, e00797-19. https://doi.org/10.1128/JVI.00797-19.
4. DiazGranados, C.A., Denis, M., and Plotkin, S. (2012). Seasonal influenza vaccine efficacy and its determinants in children and non-elderly adults: a systematic review with meta-analyses of controlled trials. Vaccine *31*, 49–57. https://doi.org/10.1016/j.vaccine.2012.10.084.
5. Arregoces-Castillo, L., Fernandez-Nino, J., Rojas-Botero, M., Palacios-Clavijo, A., Galvis-Pedraza, M., Rincon-Medrano, L., Pinto-Alvarez, M., Ruiz-Gomez, F., and Trejo-Valdivia, B. (2022). Effectiveness of COVID-19 vaccines in older adults in Colombia: a retrospective, population-based study of the ESPERANZA cohort. Lancet Healthy Longev. *3*, e242–e252. https://doi.org/10.1016/S2666-7568(22)00035-6.
6. Shao, W., Chen, X., Zheng, C., Liu, H., Wang, G., Zhang, B., Li, Z., and Zhang, W. (2022). Effectiveness of COVID-19 vaccines against SARS-CoV-2 variants of concern in real-world: a literature review and meta-analysis. Emerg. Microb. Infect. *11*, 2383–2392. https://doi.org/10.1080/22221751.2022.2122582.
7. Nanishi, E., Levy, O., and Ozonoff, A. (2022). Waning effectiveness of SARS-CoV-2 mRNA vaccines in older adults: a rapid review. Hum. Vaccines Immunother. *18*, 2045857. https://doi.org/10.1080/21645515.2022.2045857.
8. Dowling, D.J., and Levy, O. (2022). A Precision Adjuvant Approach to Enhance Severe Acute Respiratory Syndrome Coronavirus 2 (SARS-CoV-2) Vaccines Optimized for Immunologically Distinct Vulnerable Populations. Clin. Infect. Dis. *75*, S30–S36. https://doi.org/10.1093/cid/ciac342.
9. Nanishi, E., Angelidou, A., Rotman, C., Dowling, D.J., Levy, O., and Ozonoff, A. (2022). Precision Vaccine Adjuvants for Older Adults: A Scoping Review. Clin. Infect. Dis. *75*, S72–S80. https://doi.org/10.1093/cid/ciac302.
10. Amanat, F., and Krammer, F. (2020). SARS-CoV-2 Vaccines: Status Report. Immunity *52*, 583–589. https://doi.org/10.1016/j.immuni.2020.03.007.
11. Jeffery-Smith, A., Burton, A.R., Lens, S., Rees-Spear, C., Davies, J., Patel, M., Gopal, R., Muir, L., Aiano, F., Doores, K.J., et al. (2022). SARS-CoV-2-specific memory B cells can persist in the elderly who have lost detectable neutralizing antibodies. J. Clin. Invest. *132*, e152042. https://doi.org/10.1172/JCI152042.
12. Naaber, P., Tserel, L., Kangro, K., Sepp, E., Jürjenson, V., Adamson, A., Haljasmägi, L., Rumm, A.P., Maruste, R., Kärner, J., et al. (2021). Dynamics of antibody response to BNT162b2 vaccine after six months: a longitudinal prospective study. Lancet Reg. Health. Eur. *10*, 100208. https://doi.org/10.1016/j.lanepe.2021.100208.
13. Muller, L., Andree, M., Moskorz, W., Drexler, I., Walotka, L., Grothmann, R., Ptok, J., Hillebrandt, J., Ritchie, A., Rabl, D., et al. (2021). Age-dependent Immune Response to the Biontech/Pfizer BNT162b2 Coronavirus Disease 2019 Vaccination. Clin. Infect. Dis. *73*, 2065–2072. https://doi.org/10.1093/cid/ciab381.
14. Collier, D.A., Ferreira, I.A.T.M., Kotagiri, P., Datir, R.P., Lim, E.Y., Touizer, E., Meng, B., Abdullahi, A.; CITIID-NIHR BioResource COVID-19 Collaboration, and Elmer, A., et al. (2021). Age-related immune response heterogeneity to SARS-CoV-2 vaccine BNT162b2. Nature *596*, 417–422. https://doi.org/10.1038/s41586-021-03739-1.
15. Palacios-Pedrero, M.Á., Jansen, J.M., Blume, C., Stanislawski, N., Jonczyk, R., Molle, A., Hernandez, M.G., Kaiser, F.K., Jung, K., Osterhaus, A.D.M.E., et al. (2022). Signs of immunosenescence correlate with poor outcome of mRNA COVID-19 vaccination in older adults. Nat. Aging *2*, 896–905. https://doi.org/10.1038/s43587-022-00292-y.
16. Bates, T.A., Lu, P., Kang, Y.J., Schoen, D., Thornton, M., McBride, S.K., Park, C., Kim, D., Messer, W.B., Curlin, M.E., et al. (2022). BNT162b2 induced neutralizing and non-neutralizing antibody functions against SARSCoV-2 diminish with age. Preprint at medRxiv. https://doi.org/10.1101/2022.08.12.22278726.
17. Yamashita, K., Suzuki, A., Takebayashi, S., Toguchi, A., Ogitani, K., Niizeki, N., Nagura, O., Furuhashi, K., Iwaizumi, M., and Maekawa, M. (2022). Differential Dynamics of Humoral and Cell-Mediated Immunity with Three Doses of BNT162b2 SARS-CoV-2 Vaccine in Healthcare Workers in Japan: A Prospective Cohort Study. Vaccines *10*, 1050. https://doi.org/10.3390/vaccines10071050.
18. Romero-Olmedo, A.J., Schulz, A.R., Hochstätter, S., Das Gupta, D., Virta, I., Hirseland, H., Staudenraus, D., Camara, B., Münch, C., Hefter, V., et al. (2022). Induction of robust cellular and humoral immunity against SARS-CoV-2 after a third dose of BNT162b2 vaccine in previously unresponsive older adults. Nat. Microbiol. *7*, 195–199. https://doi.org/10.1038/s41564-021-01046-z.
19. Frasca, D., Riley, R.L., and Blomberg, B.B. (2005). Humoral immune response and B-cell functions including immunoglobulin class switch are downregulated in aged mice and humans. Semin. Immunol. *17*, 378–384. https://doi.org/10.1016/j.smim.2005.05.005.
20. Bulut, O., Kilic, G., Domínguez-Andrés, J., and Netea, M.G. (2020). Overcoming immune dysfunction in the elderly: trained immunity as a novel approach. Int. Immunol. *32*, 741–753. https://doi.org/10.1093/intimm/dxaa052.
21. Frasca, D., Landin, A.M., Lechner, S.C., Ryan, J.G., Schwartz, R., Riley, R.L., and Blomberg, B.B. (2008). Aging down-regulates the transcription factor E2A, activation-induced cytidine deaminase, and Ig class switch in human B cells. J. Immunol. *180*, 5283–5290. https://doi.org/10.4049/jimmunol.180.8.5283.
22. Sage, P.T., Tan, C.L., Freeman, G.J., Haigis, M., and Sharpe, A.H. (2015). Defective TFH Cell Function and Increased TFR Cells Contribute to Defective Antibody Production in Aging. Cell Rep. *12*, 163–171. https://doi.org/10.1016/j.celrep.2015.06.015.
23. Eaton, S.M., Burns, E.M., Kusser, K., Randall, T.D., and Haynes, L. (2004). Age-related defects in CD4 T cell cognate helper function lead to reductions in humoral responses. J. Exp. Med. *200*, 1613–1622. https://doi.org/10.1084/jem.20041395.

24. Gallerani, E., Proietto, D., Dallan, B., Campagnaro, M., Pacifico, S., Albanese, V., Marzola, E., Marconi, P., Caputo, A., Appay, V., et al. (2021). Impaired Priming of SARS-CoV-2-Specific Naive CD8(+) T Cells in Older Subjects. Front. Immunol. *12*, 693054. https://doi.org/10.3389/fimmu.2021.693054.
25. Westmeier, J., Paniskaki, K., Karakose, Z., Werner, T., Sutter, K., Dolff, S., Overbeck, M., Limmer, A., Liu, J., Zheng, X., et al. (2020). Impaired Cytotoxic CD8(+) T Cell Response in Elderly COVID-19 Patients. mBio *11*, e02243-20. https://doi.org/10.1128/mBio.02243-20.
26. Pellini, R., Venuti, A., Pimpinelli, F., Abril, E., Blandino, G., Campo, F., Conti, L., De Virgilio, A., De Marco, F., Di Domenico, E.G., et al. (2021). Early Onset of SARS-COV-2 Antibodies after First Dose of BNT162b2: Correlation with Age, Gender and BMI. Vaccines *9*, 685. https://doi.org/10.3390/vaccines9070685.
27. Haynes, L. (2020). Aging of the Immune System: Research Challenges to Enhance the Health Span of Older Adults. Front. Aging *1*, 602108. https://doi.org/10.3389/fragi.2020.602108.
28. Vitalle, J., Perez-Gomez, A., Ostos, F.J., Gasca-Capote, C., Jimenez-Leon, M.R., Bachiller, S., Rivas-Jeremias, I., Silva-Sanchez, M.D.M., Ruiz-Mateos, A.M., Martin-Sanchez, M.A., et al. (2022). Immune defects associated with lower SARS-CoV-2 BNT162b2 mRNA vaccine response in aged people. JCI Insight *7*, e161045. https://doi.org/10.1172/jci.insight.161045.
29. Rydyznski Moderbacher, C., Ramirez, S.I., Dan, J.M., Grifoni, A., Hastie, K.M., Weiskopf, D., Belanger, S., Abbott, R.K., Kim, C., Choi, J., et al. (2020). Antigen-Specific Adaptive Immunity to SARS-CoV-2 in Acute COVID-19 and Associations with Age and Disease Severity. Cell *183*, 996–1012.e19. https://doi.org/10.1016/j.cell.2020.09.038.
30. Vanshylla, K., Tober-Lau, P., Gruell, H., Münn, F., Eggeling, R., Pfeifer, N., Le, N.H., Landgraf, I., Kurth, F., Sander, L.E., and Klein, F. (2022). Durability of omicron-neutralising serum activity after mRNA booster immunisation in older adults. Lancet Infect. Dis. *22*, 445–446. https://doi.org/10.1016/S1473-3099(22)00135-9.
31. Lassauniere, R., Polacek, C., Frische, A., Boding, L., Saekmose, S.G., Rasmussen, M., and Fomsgaard, A. (2022). Neutralizing Antibodies Against the SARS-CoV-2 Omicron Variant (BA.1) 1 to 18 Weeks After the Second and Third Doses of the BNT162b2 mRNA Vaccine. JAMA Netw. Open *5*, e2212073. https://doi.org/10.1001/jamanetworkopen.2022.12073.
32. (2022). Coronavirus (COVID-19) Update: FDA Authorizes Second Booster Dose of Two COVID-19 Vaccines for Older and Immunocompromised Individuals. https://web.archive.org/web/20221028163104/https://www.fda.gov/news-events/press-announcements/coronavirus-covid-19-update-fda-authorizes-second-booster-dose-two-covid-19-vaccines-older.
33. Panagiotakopoulos, L., Godfrey, M., Moulia, D.L., Link-Gelles, R., Taylor, C.A., Chatham-Stephens, K., Brooks, O., Daley, M.F., Fleming-Dutra, K.E., and Wallace, M. (2024). Use of an Additional Updated 2023-2024 COVID-19 Vaccine Dose for Adults Aged >/=65 Years: Recommendations of the Advisory Committee on Immunization Practices - United States, 2024. MMWR Morb. Mortal. Wkly. Rep. *73*, 377–381. https://doi.org/10.15585/mmwr.mm7316a4.
34. Morrocchi, E., van Haren, S., Palma, P., and Levy, O. (2024). Modeling human immune responses to vaccination in vitro. Trends Immunol. *45*, 32–47. https://doi.org/10.1016/j.it.2023.11.002.
35. Dowling, D.J., van Haren, S.D., Scheid, A., Bergelson, I., Kim, D., Mancuso, C.J., Foppen, W., Ozonoff, A., Fresh, L., Theriot, T.B., et al. (2017). TLR7/8 adjuvant overcomes newborn hyporesponsiveness to pneumococcal conjugate vaccine at birth. JCI Insight *2*, e91020. https://doi.org/10.1172/jci.insight.91020.
36. Sanchez-Schmitz, G., Stevens, C.R., Bettencourt, I.A., Flynn, P.J., Schmitz-Abe, K., Metser, G., Hamm, D., Jensen, K.J., Benn, C., and Levy, O. (2018). Microphysiologic Human Tissue Constructs Reproduce Autologous Age-Specific BCG and HBV Primary Immunization in vitro. Front. Immunol. *9*, 2634. https://doi.org/10.3389/fimmu.2018.02634.
37. Zushin, P.J.H., Mukherjee, S., and Wu, J.C. (2023). FDA Modernization Act 2.0: transitioning beyond animal models with human cells, organoids, and AI/ML-based approaches. J. Clin. Invest. *133*, e175824. https://doi.org/10.1172/JCI175824.
38. Giacomini, E., Iona, E., Ferroni, L., Miettinen, M., Fattorini, L., Orefici, G., Julkunen, I., and Coccia, E.M. (2001). Infection of human macrophages and dendritic cells with Mycobacterium tuberculosis induces a differential cytokine gene expression that modulates T cell response. J. Immunol. *166*, 7033–7041. https://doi.org/10.4049/jimmunol.166.12.7033.
39. Højsgaard, S., Halekoh, U., and Yan, J. (2005). The R Package geepack for Generalized Estimating Equations. J. Stat. Software *15*, 1–11. https://doi.org/10.18637/jss.v015.i02.
40. Buzkova, P., Brown, E.R., and John-Stewart, G.C. (2010). Longitudinal data analysis for generalized linear models under participant-driven informative follow-up: an application in maternal health epidemiology. Am. J. Epidemiol. *171*, 189–197. https://doi.org/10.1093/aje/kwp353.
41. Prentice, R.L., and Zhao, L.P. (1991). Estimating equations for parameters in means and covariances of multivariate discrete and continuous responses. Biometrics *47*, 825–839.
42. Roubinian, N.H., Plimier, C., Woo, J.P., Lee, C., Bruhn, R., Liu, V.X., Escobar, G.J., Kleinman, S.H., Triulzi, D.J., Murphy, E.L., and Busch, M.P. (2019). Effect of donor, component, and recipient characteristics on hemoglobin increments following red blood cell transfusion. Blood *134*, 1003–1013. https://doi.org/10.1182/blood.2019000773.
43. Carson, W.F., 4th, Salter-Green, S.E., Scola, M.M., Joshi, A., Gallagher, K.A., and Kunkel, S.L. (2017). Enhancement of macrophage inflammatory responses by CCL2 is correlated with increased miR-9 expression and downregulation of the ERK1/2 phosphatase Dusp6. Cell. Immunol. *314*, 63–72. https://doi.org/10.1016/j.cellimm.2017.02.005.
44. Chang, T.T., and Chen, J.W. (2016). Emerging role of chemokine CC motif ligand 4 related mechanisms in diabetes mellitus and cardiovascular disease: friends or foes? Cardiovasc. Diabetol. *15*, 117. https://doi.org/10.1186/s12933-016-0439-9.
45. Ford, J., Hughson, A., Lim, K., Bardina, S.V., Lu, W., Charo, I.F., Lim, J.K., and Fowell, D.J. (2018). CCL7 Is a Negative Regulator of Cutaneous Inflammation Following Leishmania major Infection. Front. Immunol. *9*, 3063. https://doi.org/10.3389/fimmu.2018.03063.
46. Ji, J., Wang, P., Zhou, Q., Zhu, L., Zhang, H., Zhang, Y., Zheng, Z., Bhatta, A.K., Zhang, G., and Wang, X. (2019). CCL8 enhances sensitivity of cutaneous squamous cell carcinoma to photodynamic therapy by recruiting M1 macrophages. Photodiagnosis Photodyn. Ther. *26*, 235–243. https://doi.org/10.1016/j.pdpdt.2019.03.014.
47. Ma, J., Chan, C.C., Huang, W.C., and Kuo, M.L. (2020). Berberine Inhibits Pro-inflammatory Cytokine-induced IL-6 and CCL11 Production via Modulation of STAT6 Pathway in Human Bronchial Epithelial Cells. Int. J. Med. Sci. *17*, 1464–1473. https://doi.org/10.7150/ijms.45400.
48. Campbell, L.M., Maxwell, P.J., and Waugh, D.J.J. (2013). Rationale and Means to Target Pro-Inflammatory Interleukin-8 (CXCL8) Signaling in Cancer. Pharmaceuticals *6*, 929–959. https://doi.org/10.3390/ph6080929.
49. Dinarello, C.A. (1996). Biologic basis for interleukin-1 in disease. Blood *87*, 2095–2147.
50. Odak, I., Riemann, L., Sandrock, I., Cossmann, A., Ramos, G.M., Hammerschmidt, S.I., Ritter, C., Friedrichsen, M., Hassan, A., Dopfer-Jablonka, A., et al. (2024). Systems biology analysis reveals distinct molecular signatures associated with immune responsiveness to the BNT162b COVID-19 vaccine. EBioMedicine *99*, 104947. https://doi.org/10.1016/j.ebiom.2023.104947.
51. Firacative, C., Gressler, A.E., Schubert, K., Schulze, B., Müller, U., Brombacher, F., von Bergen, M., and Alber, G. (2018). Identification of T helper (Th)1- and Th2-associated antigens of Cryptococcus neoformans in a murine model of pulmonary infection. Sci. Rep. *8*, 2681. https://doi.org/10.1038/s41598-018-21039-z.
52. Tangye, S.G., Burnett, D.L., and Bull, R.A. (2022). Getting to the (germinal) center of humoral immune responses to SARS-CoV-2. Cell *185*, 945–948. https://doi.org/10.1016/j.cell.2022.02.018.
53. Earle, K.A., Ambrosino, D.M., Fiore-Gartland, A., Goldblatt, D., Gilbert, P.B., Siber, G.R., Dull, P., and Plotkin, S.A. (2021). Evidence for antibody as a protective correlate for COVID-19 vaccines. Vaccine *39*, 4423–4428. https://doi.org/10.1016/j.vaccine.2021.05.063.
54. Zhou, F., Vahokoski, J., Bergen COVID-19 Research Group, Langeland, N., and Cox, R.J. (2024). Impact of ageing on homologous and human-coronavirus-reactive antibodies after SARS-CoV-2 vaccination or infection. NPJ Vaccines *9*, 37. https://doi.org/10.1038/s41541-024-00817-z.
55. Zhou, F., Yu, T., Du, R., Fan, G., Liu, Y., Liu, Z., Xiang, J., Wang, Y., Song, B., Gu, X., et al. (2020). Clinical course and risk factors for mortality of adult inpatients with COVID-19 in Wuhan, China: a retrospective cohort

study. Lancet *395*, 1054–1062. https://doi.org/10.1016/S0140-6736(20)30566-3.
56. Bates, T.A., Lu, P., Kang, Y.J., Schoen, D., Thornton, M., McBride, S.K., Park, C., Kim, D., Messer, W.B., Curlin, M.E., et al. (2022). BNT162b2-induced neutralizing and non-neutralizing antibody functions against SARS-CoV-2 diminish with age. Cell Rep. *41*, 111544. https://doi.org/10.1016/j.celrep.2022.111544.
57. Buschmann, M.D., Carrasco, M.J., Alishetty, S., Paige, M., Alameh, M.G., and Weissman, D. (2021). Nanomaterial Delivery Systems for mRNA Vaccines. Vaccines *9*, 65. https://doi.org/10.3390/vaccines9010065.
58. (2022). Learning lessons from lipids to make COVID-19 vaccines. Cell *185*, 1279–1282. https://doi.org/10.1016/j.cell.2022.03.026.
59. Alameh, M.G., Tombacz, I., Bettini, E., Lederer, K., Sittplangkoon, C., Wilmore, J.R., Gaudette, B.T., Soliman, O.Y., Pine, M., Hicks, P., et al. (2021). Lipid nanoparticles enhance the efficacy of mRNA and protein subunit vaccines by inducing robust T follicular helper cell and humoral responses. Immunity *54*, 2877–2892.e2877. https://doi.org/10.1016/j.immuni.2021.11.001.
60. Huang, X., Kong, N., Zhang, X., Cao, Y., Langer, R., and Tao, W. (2022). The landscape of mRNA nanomedicine. Nat. Med. *28*, 2273–2287. https://doi.org/10.1038/s41591-022-02061-1.
61. Borriello, F., van Haren, S.D., and Levy, O. (2018). First International Precision Vaccines Conference: Multidisciplinary Approaches to Next-Generation Vaccines. mSphere *3*, e00214-18. https://doi.org/10.1128/mSphere.00214-18.
62. Barman, S., Soni, D., Brook, B., Nanishi, E., and Dowling, D.J. (2021). Precision Vaccine Development: Cues From Natural Immunity. Front. Immunol. *12*, 662218. https://doi.org/10.3389/fimmu.2021.662218.
63. Gupta, N., Vedi, S., Kunimoto, D.Y., Agrawal, B., and Kumar, R. (2016). Novel lipopeptides of ESAT-6 induce strong protective immunity against Mycobacterium tuberculosis: Routes of immunization and TLR agonists critically impact vaccine's efficacy. Vaccine *34*, 5677–5688. https://doi.org/10.1016/j.vaccine.2016.08.075.
64. Salleh, M.Z., Norazmi, M.N., and Deris, Z.Z. (2022). Immunogenicity mechanism of mRNA vaccines and their limitations in promoting adaptive protection against SARS-CoV-2. PeerJ *10*, e13083. https://doi.org/10.7717/peerj.13083.
65. Khan, S., Shafiei, M.S., Longoria, C., Schoggins, J.W., Savani, R.C., and Zaki, H. (2021). SARS-CoV-2 spike protein induces inflammation via TLR2-dependent activation of the NF-κB pathway. Elife *10*, e68563. https://doi.org/10.7554/eLife.68563.
66. Zhao, Y., Kuang, M., Li, J., Zhu, L., Jia, Z., Guo, X., Hu, Y., Kong, J., Yin, H., Wang, X., and You, F. (2021). SARS-CoV-2 spike protein interacts with and activates TLR4. Cell Res. *31*, 818–820. https://doi.org/10.1038/s41422-021-00495-9.
67. Sun, Y., Ishibashi, M., Seimon, T., Lee, M., Sharma, S.M., Fitzgerald, K.A., Samokhin, A.O., Wang, Y., Sayers, S., Aikawa, M., et al. (2009). Free cholesterol accumulation in macrophage membranes activates Toll-like receptors and p38 mitogen-activated protein kinase and induces cathepsin K. Circ. Res. *104*, 455–465. https://doi.org/10.1161/CIRCRESAHA.108.182568.
68. Rebendenne, A., Valadao, A.L.C., Tauziet, M., Maarifi, G., Bonaventure, B., McKellar, J., Planes, R., Nisole, S., Arnaud-Arnould, M., Moncorge, O., and Goujon, C. (2021). SARS-CoV-2 triggers an MDA-5-dependent interferon response which is unable to control replication in lung epithelial cells. J. Virol. *95*, e02415-20. https://doi.org/10.1128/JVI.02415-20.
69. Koyama, S., Aoshi, T., Tanimoto, T., Kumagai, Y., Kobiyama, K., Tougan, T., Sakurai, K., Coban, C., Horii, T., Akira, S., and Ishii, K.J. (2010). Plasmacytoid dendritic cells delineate immunogenicity of influenza vaccine subtypes. Sci. Transl. Med. *2*, 25ra24. https://doi.org/10.1126/scitranslmed.3000759.
70. Chen, T.T., Tan, L.R., Hu, N., Dong, Z.Q., Hu, Z.G., Jiang, Y.M., Chen, P., Pan, M.H., and Lu, C. (2018). C-lysozyme contributes to antiviral immunity in Bombyx mori against nucleopolyhedrovirus infection. J. Insect Physiol. *108*, 54–60. https://doi.org/10.1016/j.jinsphys.2018.05.005.
71. Yan, B., Freiwald, T., Chauss, D., Wang, L., West, E., Mirabelli, C., Zhang, C.J., Nichols, E.M., Malik, N., Gregory, R., et al. (2021). SARS-CoV-2 drives JAK1/2-dependent local complement hyperactivation. Sci. Immunol. *6*, eabg0833. https://doi.org/10.1126/sciimmunol.abg0833.
72. Mann, J.K., and Ndung'u, T. (2020). The potential of lactoferrin, ovotransferrin and lysozyme as antiviral and immune-modulating agents in COVID-19. Future Virol. *15*, 609–624. https://doi.org/10.2217/fvl-2020-0170.
73. Leng, L., Ma, J., Zhang, P.P., Xu, S.C., Li, X., Jin, Y., Cai, J., Tang, R., Zhao, L., He, Z.C., et al. (2022). Spatial region-resolved proteome map reveals mechanism of COVID-19-associated heart injury. Cell Rep. *39*, 110955. https://doi.org/10.1016/j.celrep.2022.110955.
74. Carapito, R., Li, R., Helms, J., Carapito, C., Gujja, S., Rolli, V., Guimaraes, R., Malagon-Lopez, J., Spinnhirny, P., Lederle, A., et al. (2022). Identification of driver genes for critical forms of COVID-19 in a deeply phenotyped young patient cohort. Sci. Transl. Med. *14*, eabj7521. https://doi.org/10.1126/scitranslmed.abj7521.
75. Gutmann, C., Takov, K., Burnap, S.A., Singh, B., Ali, H., Theofilatos, K., Reed, E., Hasman, M., Nabeebaccus, A., Fish, M., et al. (2021). SARS-CoV-2 RNAemia and proteomic trajectories inform prognostication in COVID-19 patients admitted to intensive care. Nat. Commun. *12*, 3406. https://doi.org/10.1038/s41467-021-23494-1.
76. Bergsneider, B., Bailey, E., Ahmed, Y., Gogineni, N., Huntley, D., and Montano, X. (2021). Analysis of SARS-CoV-2 infection associated cell entry proteins ACE2, CD147, PPIA, and PPIB in datasets from non SARS-CoV-2 infected neuroblastoma patients, as potential prognostic and infection biomarkers in neuroblastoma. Biochem. Biophys. Rep. *27*, 101081. https://doi.org/10.1016/j.bbrep.2021.101081.
77. Klotman, M.E., and Chang, T.L. (2006). Defensins in innate antiviral immunity. Nat. Rev. Immunol. *6*, 447–456. https://doi.org/10.1038/nri1860.
78. Chen, H., Liu, W., Wang, Y., Liu, D., Zhao, L., and Yu, J. (2021). SARS-CoV-2 activates lung epithelial cell proinflammatory signaling and leads to immune dysregulation in COVID-19 patients. EBioMedicine *70*, 103500. https://doi.org/10.1016/j.ebiom.2021.103500.
79. Mast, A.E., Wolberg, A.S., Gailani, D., Garvin, M.R., Alvarez, C., Miller, J.I., Aronow, B., and Jacobson, D. (2021). SARS-CoV-2 suppresses anticoagulant and fibrinolytic gene expression in the lung. Elife *10*, e64330. https://doi.org/10.7554/eLife.64330.
80. Li, H., Xiang, X., Ren, H., Xu, L., Zhao, L., Chen, X., Long, H., Wang, Q., and Wu, Q. (2020). Serum Amyloid A is a biomarker of severe Coronavirus Disease and poor prognosis. J. Infect. *80*, 646–655. https://doi.org/10.1016/j.jinf.2020.03.035.
81. Ciccosanti, F., Antonioli, M., Sacchi, A., Notari, S., Farina, A., Beccacece, A., Fusto, M., Vergori, A., D'Offizi, G., Taglietti, F., et al. (2022). Proteomic analysis identifies a signature of disease severity in the plasma of COVID-19 pneumonia patients associated to neutrophil, platelet and complement activation. Clin. Proteonomics *19*, 38. https://doi.org/10.1186/s12014-022-09377-7.
82. Delorey, T.M., Ziegler, C.G.K., Heimberg, G., Normand, R., Yang, Y., Segerstolpe, A., Abbondanza, D., Fleming, S.J., Subramanian, A., Montoro, D.T., et al. (2021). A single-cell and spatial atlas of autopsy tissues reveals pathology and cellular targets of SARS-CoV-2. Preprint at bioRxiv. https://doi.org/10.1101/2021.02.25.430130.
83. Kluck, G.E.G., Yoo, J.A., Sakarya, E.H., and Trigatti, B.L. (2021). Good Cholesterol Gone Bad? HDL and COVID-19. Int. J. Mol. Sci. *22*, 10182. https://doi.org/10.3390/ijms221910182.
84. Costanzo, M., Caterino, M., Fedele, R., Cevenini, A., Pontillo, M., Barra, L., and Ruoppolo, M. (2022). COVIDomics: The Proteomic and Metabolomic Signatures of COVID-19. Int. J. Mol. Sci. *23*, 2414. https://doi.org/10.3390/ijms23052414.
85. Liu, J., Zhang, X., Cheng, Y., and Cao, X. (2021). Dendritic cell migration in inflammation and immunity. Cell. Mol. Immunol. *18*, 2461–2471. https://doi.org/10.1038/s41423-021-00726-4.
86. Lee, A., Scott, M.K.D., Wimmers, F., Arunachalam, P.S., Luo, W., Fox, C.B., Tomai, M., Khatri, P., and Pulendran, B. (2022). A molecular atlas of innate immunity to adjuvanted and live attenuated vaccines, in mice. Nat. Commun. *13*, 549. https://doi.org/10.1038/s41467-022-28197-9.
87. Simons, R.J., and Reynolds, H.Y. (1990). Altered immune status in the elderly. Semin. Respir. Infect. *5*, 251–259.
88. Cunha, L.L., Perazzio, S.F., Azzi, J., Cravedi, P., and Riella, L.V. (2020). Remodeling of the Immune Response With Aging: Immunosenescence and Its Potential Impact on COVID-19 Immune Response. Front. Immunol. *11*, 1748. https://doi.org/10.3389/fimmu.2020.01748.
89. McCormick, S.M., and Heller, N.M. (2015). Commentary: IL-4 and IL-13 receptors and signaling. Cytokine *75*, 38–50. https://doi.org/10.1016/j.cyto.2015.05.023.
90. Takeuchi, A., Badr, M.E.S.G., Miyauchi, K., Ishihara, C., Onishi, R., Guo, Z., Sasaki, Y., Ike, H., Takumi, A., Tsuji, N.M., et al. (2016). CRTAM determines the CD4+ cytotoxic T lymphocyte lineage. J. Exp. Med. *213*, 123–138. https://doi.org/10.1084/jem.20150519.

91. Tahtinen, S., Tong, A.J., Himmels, P., Oh, J., Paler-Martinez, A., Kim, L., Wichner, S., Oei, Y., McCarron, M.J., Freund, E.C., et al. (2022). IL-1 and IL-1ra are key regulators of the inflammatory response to RNA vaccines. Nat. Immunol. *23*, 532–542. https://doi.org/10.1038/s41590-022-01160-y.
92. Barmada, A., Klein, J., Ramaswamy, A., Brodsky, N.N., Jaycox, J.R., Sheikha, H., Jones, K.M., Habet, V., Campbell, M., Sumida, T.S., et al. (2023). Cytokinopathy with aberrant cytotoxic lymphocytes and profibrotic myeloid response in SARS-CoV-2 mRNA vaccine-associated myocarditis. Sci. Immunol. *8*, eadh3455. https://doi.org/10.1126/sciimmunol.adh3455.
93. Oyebanji, O.A., Wilson, B., Keresztesy, D., Carias, L., Wilk, D., Payne, M., Aung, H., Denis, K.S., Lam, E.C., Rowley, C.F., et al. (2021). Does a lack of vaccine side effects correlate with reduced BNT162b2 mRNA vaccine response among healthcare workers and nursing home residents? Aging Clin. Exp. Res. *33*, 3151–3160. https://doi.org/10.1007/s40520-021-01987-9.
94. Reichmuth, A.M., Oberli, M.A., Jaklenec, A., Langer, R., and Blankschtein, D. (2016). mRNA vaccine delivery using lipid nanoparticles. Ther. Deliv. *7*, 319–334. https://doi.org/10.4155/tde-2016-0006.
95. Zhang, Z., Mateus, J., Coelho, C.H., Dan, J.M., Moderbacher, C.R., Gálvez, R.I., Cortes, F.H., Grifoni, A., Tarke, A., Chang, J., et al. (2022). Humoral and cellular immune memory to four COVID-19 vaccines. Preprint at bioRxiv. https://doi.org/10.1101/2022.03.18.484953.
96. Muller, M., Volzke, J., Subin, B., Muller, S., Sombetzki, M., Reisinger, E.C., and Muller-Hilke, B. (2022). Single-dose SARS-CoV-2 vaccinations with either BNT162b2 or AZD1222 induce disparate Th1 responses and IgA production. BMC Med. *20*, 29. https://doi.org/10.1186/s12916-022-02240-4.
97. Farkash, I., Feferman, T., Cohen-Saban, N., Avraham, Y., Morgenstern, D., Mayuni, G., Barth, N., Lustig, Y., Miller, L., Shouval, D.S., et al. (2021). Anti-SARS-CoV-2 antibodies elicited by COVID-19 mRNA vaccine exhibit a unique glycosylation pattern. Cell Rep. *37*, 110114. https://doi.org/10.1016/j.celrep.2021.110114.
98. Kawasaki, Y., Suzuki, J., Sakai, N., Isome, M., Nozawa, R., Tanji, M., and Suzuki, H. (2004). Evaluation of T helper-1/-2 balance on the basis of IgG subclasses and serum cytokines in children with glomerulonephritis. Am. J. Kidney Dis. *44*, 42–49. https://doi.org/10.1053/j.ajkd.2004.03.029.
99. Patil, H.P., Rane, P.S., Shrivastava, S., Palkar, S., Lalwani, S., Mishra, A.C., and Arankalle, V.A. (2021). Antibody (IgA, IgG, and IgG Subtype) Responses to SARS-CoV-2 in Severe and Nonsevere COVID-19 Patients. Viral Immunol. *34*, 201–209. https://doi.org/10.1089/vim.2020.0321.
100. Jo, N., Hidaka, Y., Kikuchi, O., Fukahori, M., Sawada, T., Aoki, M., Yamamoto, M., Nagao, M., Morita, S., Nakajima, T.E., et al. (2022). Delayed antigen-specific CD4+ T-cell induction correlates with impaired immune responses to SARS-COV-2 mRNA vaccination in the elderly. Preprint at bioRxiv. https://doi.org/10.1101/2022.05.10.490700.
101. Das, G., Sheridan, S., and Janeway, C.A., Jr. (2001). The source of early IFN-gamma that plays a role in Th1 priming. J. Immunol. *167*, 2004–2010. https://doi.org/10.4049/jimmunol.167.4.2004.
102. Arora, P., Moll, J.M., Andersen, D., Workman, C.T., Williams, A.R., Kristiansen, K., and Brix, S. (2020). Body fluid from the parasitic worm Ascaris suum inhibits broad-acting pro-inflammatory programs in dendritic cells. Immunology *159*, 322–334. https://doi.org/10.1111/imm.13151.
103. Rotondi, M., Chiovato, L., Romagnani, S., Serio, M., and Romagnani, P. (2007). Role of chemokines in endocrine autoimmune diseases. Endocr. Rev. *28*, 492–520. https://doi.org/10.1210/er.2006-0044.
104. Li, J., Ge, M., Lu, S., Shi, J., Li, X., Wang, M., Huang, J., Shao, Y., Huang, Z., Zhang, J., et al. (2017). Pro-inflammatory effects of the Th1 chemokine CXCL10 in acquired aplastic anaemia. Cytokine *94*, 45–51. https://doi.org/10.1016/j.cyto.2017.04.010.
105. Laufer, J.M., and Legler, D.F. (2018). Beyond migration-Chemokines in lymphocyte priming, differentiation, and modulating effector functions. J. Leukoc. Biol. *104*, 301–312. https://doi.org/10.1002/JLB.2MR1217-494R.
106. Bosch-Camos, L., Alonso, U., Esteve-Codina, A., Chang, C.Y., Martin-Mur, B., Accensi, F., Munoz, M., Navas, M.J., Dabad, M., Vidal, E., et al. (2022). Cross-protection against African swine fever virus upon intranasal vaccination is associated with an adaptive-innate immune crosstalk. PLoS Pathog. *18*, e1010931. https://doi.org/10.1371/journal.ppat.1010931.
107. Elser, B., Lohoff, M., Kock, S., Giaisi, M., Kirchhoff, S., Krammer, P.H., and Li-Weber, M. (2002). IFN-gamma represses IL-4 expression via IRF-1 and IRF-2. Immunity *17*, 703–712. https://doi.org/10.1016/s1074-7613(02)00471-5.
108. Dufour, J.H., Dziejman, M., Liu, M.T., Leung, J.H., Lane, T.E., and Luster, A.D. (2002). IFN-gamma-inducible protein 10 (IP-10; CXCL10)-deficient mice reveal a role for IP-10 in effector T cell generation and trafficking. J. Immunol. *168*, 3195–3204. https://doi.org/10.4049/jimmunol.168.7.3195.
109. Li, C., Lee, A., Grigoryan, L., Arunachalam, P.S., Scott, M.K.D., Trisal, M., Wimmers, F., Sanyal, M., Weidenbacher, P.A., Feng, Y., et al. (2022). Mechanisms of innate and adaptive immunity to the Pfizer-BioNTech BNT162b2 vaccine. Nat. Immunol. *23*, 543–555. https://doi.org/10.1038/s41590-022-01163-9.
110. Connors, J., Joyner, D., Mege, N.J., Cusimano, G.M., Bell, M.R., Marcy, J., Taramangalam, B., Kim, K.M., Lin, P.J.C., Tam, Y.K., et al. (2023). Lipid nanoparticles (LNP) induce activation and maturation of antigen presenting cells in young and aged individuals. Commun. Biol. *6*, 188. https://doi.org/10.1038/s42003-023-04555-1.
111. Groom, J.R., Richmond, J., Murooka, T.T., Sorensen, E.W., Sung, J.H., Bankert, K., von Andrian, U.H., Moon, J.J., Mempel, T.R., and Luster, A.D. (2012). CXCR3 chemokine receptor-ligand interactions in the lymph node optimize CD4+ T helper 1 cell differentiation. Immunity *37*, 1091–1103. https://doi.org/10.1016/j.immuni.2012.08.016.
112. Yadav, D., and Sarvetnick, N. (2003). Cytokines and autoimmunity: redundancy defines their complex nature. Curr. Opin. Immunol. *15*, 697–703. https://doi.org/10.1016/j.coi.2003.09.006.
113. van Haren, S.D., Dowling, D.J., Foppen, W., Christensen, D., Andersen, P., Reed, S.G., Hershberg, R.M., Baden, L.R., and Levy, O. (2016). Age-Specific Adjuvant Synergy: Dual TLR7/8 and Mincle Activation of Human Newborn Dendritic Cells Enables Th1 Polarization. J. Immunol. *197*, 4413–4424. https://doi.org/10.4049/jimmunol.1600282.
114. Puchta, A., Naidoo, A., Verschoor, C.P., Loukov, D., Thevaranjan, N., Mandur, T.S., Nguyen, P.S., Jordana, M., Loeb, M., Xing, Z., et al. (2016). TNF Drives Monocyte Dysfunction with Age and Results in Impaired Anti-pneumococcal Immunity. PLoS Pathog. *12*, e1005368. https://doi.org/10.1371/journal.ppat.1005368.
115. Rink, L., Cakman, I., and Kirchner, H. (1998). Altered cytokine production in the elderly. Mech. Ageing Dev. *102*, 199–209. https://doi.org/10.1016/s0047-6374(97)00153-x.
116. Pardi, N., Tuyishime, S., Muramatsu, H., Kariko, K., Mui, B.L., Tam, Y.K., Madden, T.D., Hope, M.J., and Weissman, D. (2015). Expression kinetics of nucleoside-modified mRNA delivered in lipid nanoparticles to mice by various routes. J. Contr. Release *217*, 345–351. https://doi.org/10.1016/j.jconrel.2015.08.007.
117. Vogel, A.B., Kanevsky, I., Che, Y., Swanson, K.A., Muik, A., Vormehr, M., Kranz, L.M., Walzer, K.C., Hein, S., Güler, A., et al. (2021). BNT162b vaccines protect rhesus macaques from SARS-CoV-2. Nature *592*, 283–289. https://doi.org/10.1038/s41586-021-03275-y.
118. Israelow, B., Mao, T., Klein, J., Song, E., Menasche, B., Omer, S.B., and Iwasaki, A. (2021). Adaptive immune determinants of viral clearance and protection in mouse models of SARS-CoV-2. Sci. Immunol. *6*, eabl4509. https://doi.org/10.1126/sciimmunol.abl4509.
119. Levin, E.G., Lustig, Y., Cohen, C., Fluss, R., Indenbaum, V., Amit, S., Doolman, R., Asraf, K., Mendelson, E., Ziv, A., et al. (2021). Waning Immune Humoral Response to BNT162b2 Covid-19 Vaccine over 6 Months. N. Engl. J. Med. *385*, e84. https://doi.org/10.1056/NEJMoa2114583.
120. Barbeau, D.J., Martin, J.M., Carney, E., Dougherty, E., Doyle, J.D., Dermody, T.S., Hoberman, A., Williams, J.V., Michaels, M.G., Alcorn, J.F., et al. (2022). Comparative analysis of human immune responses following SARS-CoV-2 vaccination with BNT162b2, mRNA-1273, or Ad26.COV2.S. NPJ Vaccines *7*, 77. https://doi.org/10.1038/s41541-022-00504-x.
121. Irrgang, P., Gerling, J., Kocher, K., Lapuente, D., Steininger, P., Habenicht, K., Wytopil, M., Beileke, S., Schäfer, S., Zhong, J., et al. (2023). Class switch toward noninflammatory, spike-specific IgG4 antibodies after repeated SARS-CoV-2 mRNA vaccination. Sci. Immunol. *8*, eade2798. https://doi.org/10.1126/sciimmunol.ade2798.
122. Aalberse, R.C., Stapel, S.O., Schuurman, J., and Rispens, T. (2009). Immunoglobulin G4: an odd antibody. Clin. Exp. Allergy *39*, 469–477. https://doi.org/10.1111/j.1365-2222.2009.03207.x.
123. Nanishi, E., McGrath, M.E., O'Meara, T.R., Barman, S., Yu, J., Wan, H., Dillen, C.A., Menon, M., Seo, H.S., Song, K., et al. (2022). mRNA booster vaccination protects aged mice against the SARS-CoV-2 Omicron variant. Commun. Biol. *5*, 790. https://doi.org/10.1038/s42003-022-03765-3.

124. Gorman, M.J., Patel, N., Guebre-Xabier, M., Zhu, A., Atyeo, C., Pullen, K.M., Loos, C., Goez-Gazi, Y., Carrion, R., Jr., Tian, J.H., et al. (2021). Collaboration between the Fab and Fc contribute to maximal protection against SARS-CoV-2 in nonhuman primates following NVX-CoV2373 subunit vaccine with Matrix-M vaccination. Preprint at bioRxiv. https://doi.org/10.1101/2021.02.05.429759.
125. Walsh, E.E., Frenck, R.W., Jr., Falsey, A.R., Kitchin, N., Absalon, J., Gurtman, A., Lockhart, S., Neuzil, K., Mulligan, M.J., Bailey, R., et al. (2020). Safety and Immunogenicity of Two RNA-Based Covid-19 Vaccine Candidates. N. Engl. J. Med. *383*, 2439–2450. https://doi.org/10.1056/NEJMoa2027906.
126. Altmann, D.M., and Boyton, R.J. (2020). SARS-CoV-2 T cell immunity: Specificity, function, durability, and role in protection. Sci. Immunol. *5*, eabd6160. https://doi.org/10.1126/sciimmunol.abd6160.
127. Gruell, H., Vanshylla, K., Tober-Lau, P., Hillus, D., Schommers, P., Lehmann, C., Kurth, F., Sander, L.E., and Klein, F. (2022). mRNA booster immunization elicits potent neutralizing serum activity against the SARS-CoV-2 Omicron variant. Nat. Med. *28*, 477–480. https://doi.org/10.1038/s41591-021-01676-0.
128. Liu, J., Wang, S., Liu, H., Yang, L., and Nan, G. (1995). Stimulatory effect of saponin from Panax ginseng on immune function of lymphocytes in the elderly. Mech. Ageing Dev. *83*, 43–53. https://doi.org/10.1016/0047-6374(95)01618-a.
129. Heineman, T.C., Cunningham, A., and Levin, M. (2019). Understanding the immunology of Shingrix, a recombinant glycoprotein E adjuvanted herpes zoster vaccine. Curr. Opin. Immunol. *59*, 42–48. https://doi.org/10.1016/j.coi.2019.02.009.
130. Nanishi, E., Borriello, F., O'Meara, T.R., McGrath, M.E., Saito, Y., Haupt, R.E., Seo, H.S., van Haren, S.D., Cavazzoni, C.B., Brook, B., et al. (2022). An aluminum hydroxide:CpG adjuvant enhances protection elicited by a SARS-CoV-2 receptor binding domain vaccine in aged mice. Sci. Transl. Med. *14*, eabj5305. https://doi.org/10.1126/scitranslmed.abj5305.
131. Pollet, J., Strych, U., Chen, W.H., Versteeg, L., Keegan, B., Zhan, B., Wei, J., Liu, Z., Lee, J., Kundu, R., et al. (2022). Receptor-binding domain recombinant protein on alum-CpG induces broad protection against SARS-CoV-2 variants of concern. Preprint at bioRxiv. https://doi.org/10.1101/2021.07.06.451353.
132. Salunke, D.B., and Lindsley, C.W. (2023). Call for Papers: Medicinal Chemistry of Next Generation Vaccine Adjuvants. J. Med. Chem. *66*, 10119–10121. https://doi.org/10.1021/acs.jmedchem.3c01248.
133. Raphael, I., Nalawade, S., Eagar, T.N., and Forsthuber, T.G. (2015). T cell subsets and their signature cytokines in autoimmune and inflammatory diseases. Cytokine *74*, 5–17. https://doi.org/10.1016/j.cyto.2014.09.011.
134. Ekkens, M.J., Shedlock, D.J., Jung, E., Troy, A., Pearce, E.L., Shen, H., and Pearce, E.J. (2007). Th1 and Th2 cells help CD8 T-cell responses. Infect. Immun. *75*, 2291–2296. https://doi.org/10.1128/IAI.01328-06.
135. Miyauchi, K., Sugimoto-Ishige, A., Harada, Y., Adachi, Y., Usami, Y., Kaji, T., Inoue, K., Hasegawa, H., Watanabe, T., Hijikata, A., et al. (2016). Protective neutralizing influenza antibody response in the absence of T follicular helper cells. Nat. Immunol. *17*, 1447–1458. https://doi.org/10.1038/ni.3563.
136. Pettengill, M.A., van Haren, S.D., and Levy, O. (2014). Soluble mediators regulating immunity in early life. Front. Immunol. *5*, 457. https://doi.org/10.3389/fimmu.2014.00457.
137. Vlatkovic, I. (2021). Non-Immunotherapy Application of LNP-mRNA: Maximizing Efficacy and Safety. Biomedicines *9*, 530. https://doi.org/10.3390/biomedicines9050530.
138. Pecetta, S., Tortorice, D., Scorza, F.B., Pizza, M., Dougan, G., Hatchett, R., Black, S., Bloom, D.E., and Rappuoli, R. (2022). The trillion dollar vaccine gap. Sci. Transl. Med. *14*, eabn4342. https://doi.org/10.1126/scitranslmed.abn4342.
139. Brook, B., Duval, V., Barman, S., Speciner, L., Sweitzer, C., Khanmohammed, A., Menon, M., Foster, K., Ghosh, P., Abedi, K., et al. (2024). Adjuvantation of a SARS-CoV-2 mRNA vaccine with controlled tissue-specific expression of an mRNA encoding IL-12p70. Sci. Transl. Med. *16*, eadm8451. https://doi.org/10.1126/scitranslmed.adm8451.
140. Aunins, E.A., Phan, A.T., Alameh, M.-G., Cruz-Morales, E., Christian, D.A., Bunkofske, M.E., Dwivedi, G., Kedl, R., Weissman, D., and Hunter, C.A. (2024). An IL-12 mRNA-LNP adjuvant enhances mRNA vaccine induced CD8+ T cell responses. Preprint at bioRxiv. 2024.2007.2029.605626. https://doi.org/10.1101/2024.07.29.605626.
141. Grubeck-Loebenstein, B., Della Bella, S., Iorio, A.M., Michel, J.P., Pawelec, G., and Solana, R. (2009). Immunosenescence and vaccine failure in the elderly. Aging Clin. Exp. Res. *21*, 201–209. https://doi.org/10.1007/BF03324904.
142. Garcia Verdecia, B., Saavedra Hernandez, D., Lorenzo-Luaces, P., de Jesus Badia Alvarez, T., Leonard Rupale, I., Mazorra Herrera, Z., Crombet Ramos, T., and Lage Davila, A. (2013). Immunosenescence and gender: a study in healthy Cubans. Immun. Ageing *10*, 16. https://doi.org/10.1186/1742-4933-10-16.
143. Ricke-Hoch, M., Stelling, E., Lasswitz, L., Gunesch, A.P., Kasten, M., Zapatero-Belinchón, F.J., Brogden, G., Gerold, G., Pietschmann, T., Montiel, V., et al. (2021). Impaired immune response mediated by prostaglandin E2 promotes severe COVID-19 disease. PLoS One *16*, e0255335. https://doi.org/10.1371/journal.pone.0255335.
144. Bar-On, Y.M., Goldberg, Y., Mandel, M., Bodenheimer, O., Amir, O., Freedman, L., Alroy-Preis, S., Ash, N., Huppert, A., and Milo, R. (2022). Protection by a Fourth Dose of BNT162b2 against Omicron in Israel. N. Engl. J. Med. *386*, 1712–1720. https://doi.org/10.1056/NEJMoa2201570.
145. Furman, D., Jojic, V., Sharma, S., Shen-Orr, S.S., Angel, C.J.L., Onengut-Gumuscu, S., Kidd, B.A., Maecker, H.T., Concannon, P., Dekker, C.L., et al. (2015). Cytomegalovirus infection enhances the immune response to influenza. Sci. Transl. Med. *7*, 281ra43. https://doi.org/10.1126/scitranslmed.aaa2293.
146. Sayed, N., Huang, Y., Nguyen, K., Krejciova-Rajaniemi, Z., Grawe, A.P., Gao, T., Tibshirani, R., Hastie, T., Alpert, A., Cui, L., et al. (2021). An inflammatory aging clock (iAge) based on deep learning tracks multimorbidity, immunosenescence, frailty and cardiovascular aging. Nat. Aging *1*, 598–615. https://doi.org/10.1038/s43587-021-00082-y.
147. Hubbard, R.E., and Woodhouse, K.W. (2010). Frailty, inflammation and the elderly. Biogerontology *11*, 635–641. https://doi.org/10.1007/s10522-010-9292-5.
148. MacLean, B., Tomazela, D.M., Shulman, N., Chambers, M., Finney, G.L., Frewen, B., Kern, R., Tabb, D.L., Liebler, D.C., and MacCoss, M.J. (2010). Skyline: an open source document editor for creating and analyzing targeted proteomics experiments. Bioinformatics *26*, 966–968. https://doi.org/10.1093/bioinformatics/btq054.
149. R Development Core Team (2021). A Language and Environment for Statistical Computing (R Foundation for Statistical Computing). https://www.R-project.org/.
150. RStudio Team (2020). RStudio: Integrated Development for R (RStudio, PBC). http://www.rstudio.com/.
151. Pagès, H.,C.M., Falcon, S., and Li, N. (2023). AnnotationDbi: Manipulation of SQLite-based annotations in Bioconductor. https://bioconductor.org/packages/AnnotationDbi.
152. Yu, G., and He, Q.Y. (2016). ReactomePA: an R/Bioconductor package for reactome pathway analysis and visualization. Mol. Biosyst. *12*, 477–479. https://doi.org/10.1039/c5mb00663e.
153. Yu, G., Wang, L.G., Yan, G.R., and He, Q.Y. (2015). DOSE: an R/Bioconductor package for disease ontology semantic and enrichment analysis. Bioinformatics *31*, 608–609. https://doi.org/10.1093/bioinformatics/btu684.
154. Pedersen, T.L. (2022). An Implementation of Grammar of Graphics for Graphs and Networks. https://github.com/thomasp85/ggraph.
155. Søren Højsgaard, U.H., Yan, J., and Ekstrøm, C.T. (2005). The R Package geepack for Generalized Estimating Equations. J. Stat. Software *15*, 1–11. https://doi.org/10.18637/jss.v015.i02.
156. Rohart, F., Gautier, B., Singh, A., and Lê Cao, K.A. (2017). mixOmics: An R package for 'omics feature selection and multiple data integration. PLoS Comput. Biol. *13*, e1005752. https://doi.org/10.1371/journal.pcbi.1005752.
157. Ritchie, M.E., Phipson, B., Wu, D., Hu, Y., Law, C.W., Shi, W., and Smyth, G.K. (2015). limma powers differential expression analyses for RNA-sequencing and microarray studies. Nucleic Acids Res. *43*, e47. https://doi.org/10.1093/nar/gkv007.
158. Wickham, H. (2011). The Split-Apply-Combine Strategy for Data Analysis. J. Stat. Software *40*, 1–29.
159. Hadley Wickham, R.F., Henry, L., Müller, K., and Davis, V. (2023). A Grammar of Data Manipulation. https://dplyr.tidyverse.org.
160. Wickham, H. (2007). Reshaping Data with the reshape Package. J. Stat. Software *21*, 1–20.
161. Wickham, H. (2016). ggplot2: Elegant Graphics for Data Analysis (Springer-Verlag).
162. Kassambara, A. (2023). ggpubr: 'ggplot2' Based Publication Ready Plots. https://rpkgs.datanovia.com/ggpubr/.
163. Tang, Y., Horikoshi, M., and Li, W. (2016). ggfortify: Unified Interface to Visualize Statistical Result of Popular R Packages. RELC J. *8*, 474–485. https://doi.org/10.32614/RJ-2016-060.

164. Horikoshi, M., Tang, Y., Dickey, A., Grenié, M., Thompson, R., Selzer, L., Strbenac, D., Voronin, K., and Pulatov, D. (2018). ggfortify: Data Visualization Tools for Statistical Analysis Results. https://CRAN.R-project.org/package=ggfortify.
165. Pedersen, T.L. (2022). ggforce: Accelerating 'ggplot2'. https://github.com/thomasp85/ggforce.
166. Robinson, D., Hayes, A., and Couch, S. (2023). broom: Convert Statistical Objects into Tidy Tibbles. https://broom.tidymodels.org/.
167. Bion, R., Syahputra, M.A., Mendoza, P., Averick, M., Bryan, J., Chang, W., Francois, R., Grolemund, G., Hayes, A., Henry, L., et al. ggradar. https://github.com/ricardo-bion/ggradar.
168. Wickham, H., Averick, M., Bryan, J., Chang, W., D'Agostino McGowan, L., François, R., Grolemund, G., Hayes, A., Henry, L., Hester, J., et al. (2019). Welcome to the tidyverse. J. Open Source Softw. *4*, 1686. https://doi.org/10.21105/joss.01686.
169. Hadley Wickham, D.S. (2022). scales: Scale Functions for Visualization. https://scales.r-lib.org.
170. Roberts, A., Deming, D., Paddock, C.D., Cheng, A., Yount, B., Vogel, L., Herman, B.D., Sheahan, T., Heise, M., Genrich, G.L., et al. (2007). A mouse-adapted SARS-coronavirus causes disease and mortality in BALB/c mice. PLoS Pathog. *3*, e5. https://doi.org/10.1371/journal.ppat.0030005.
171. van Haren, S.D., Ganapathi, L., Bergelson, I., Dowling, D.J., Banks, M., Samuels, R.C., Reed, S.G., Marshall, J.D., and Levy, O. (2016). In vitro cytokine induction by TLR-activating vaccine adjuvants in human blood varies by age and adjuvant. Cytokine *83*, 99–109. https://doi.org/10.1016/j.cyto.2016.04.001.
172. Kollmann, T.R., Crabtree, J., Rein-Weston, A., Blimkie, D., Thommai, F., Wang, X.Y., Lavoie, P.M., Furlong, J., Fortuno, E.S., 3rd, Hajjar, A.M., et al. (2009). Neonatal innate TLR-mediated responses are distinct from those of adults. J. Immunol. *183*, 7150–7160. https://doi.org/10.4049/jimmunol.0901481.
173. Vaes, R.D.W., Reynders, K., Sprooten, J., Nevola, K.T., Rouschop, K.M.A., Vooijs, M., Garg, A.D., Lambrecht, M., Hendriks, L.E.L., Rucevic, M., and De Ruysscher, D. (2021). Identification of Potential Prognostic and Predictive Immunological Biomarkers in Patients with Stage I and Stage III Non-Small Cell Lung Cancer (NSCLC): A Prospective Exploratory Study. Cancers *13*, 6259. https://doi.org/10.3390/cancers13246259.
174. Castle, S., Uyemura, K., Wong, W., Modlin, R., and Effros, R. (1997). Evidence of enhanced type 2 immune response and impaired upregulation of a type 1 response in frail elderly nursing home residents. Mech. Ageing Dev. *94*, 7–16. https://doi.org/10.1016/s0047-6374(96)01821-0.
175. Milpied, P.J., and McHeyzer-Williams, M.G. (2013). High-affinity IgA needs TH17 cell functional plasticity. Nat. Immunol. *14*, 313–315. https://doi.org/10.1038/ni.2567.
176. Christensen, D., Mortensen, R., Rosenkrands, I., Dietrich, J., and Andersen, P. (2017). Vaccine-induced Th17 cells are established as resident memory cells in the lung and promote local IgA responses. Mucosal Immunol. *10*, 260–270. https://doi.org/10.1038/mi.2016.28.
177. Shi, G., Cox, C.A., Vistica, B.P., Tan, C., Wawrousek, E.F., and Gery, I. (2008). Phenotype switching by inflammation-inducing polarized Th17 cells, but not by Th1 cells. J. Immunol. *181*, 7205–7213. https://doi.org/10.4049/jimmunol.181.10.7205.
178. Kumar, P., Chen, K., and Kolls, J.K. (2013). Th17 cell based vaccines in mucosal immunity. Curr. Opin. Immunol. *25*, 373–380. https://doi.org/10.1016/j.coi.2013.03.011.
179. Mitchell, L.A., Henderson, A.J., and Dow, S.W. (2012). Suppression of vaccine immunity by inflammatory monocytes. J. Immunol. *189*, 5612–5621. https://doi.org/10.4049/jimmunol.1202151.
180. Rocamora-Reverte, L., Melzer, F.L., Würzner, R., and Weinberger, B. (2020). The Complex Role of Regulatory T Cells in Immunity and Aging. Front. Immunol. *11*, 616949. https://doi.org/10.3389/fimmu.2020.616949.
181. Agrawal, S., and Gupta, S. (2011). TLR1/2, TLR7, and TLR9 signals directly activate human peripheral blood naive and memory B cell subsets to produce cytokines, chemokines, and hematopoietic growth factors. J. Clin. Immunol. *31*, 89–98. https://doi.org/10.1007/s10875-010-9456-8.
182. Chen, C., Liu, Y., Liu, Y., and Zheng, P. (2009). mTOR regulation and therapeutic rejuvenation of aging hematopoietic stem cells. Sci. Signal. *2*, ra75. https://doi.org/10.1126/scisignal.2000559.
183. Ziogas, A., and Netea, M.G. (2022). Trained immunity-related vaccines: innate immune memory and heterologous protection against infections. Trends Mol. Med. *28*, 497–512. https://doi.org/10.1016/j.molmed.2022.03.009.
184. Barman, S., Borriello, F., Brook, B., Pietrasanta, C., De Leon, M., Sweitzer, C., Menon, M., van Haren, S.D., Soni, D., Saito, Y., et al. (2022). Shaping Neonatal Immunization by Tuning the Delivery of Synergistic Adjuvants via Nanocarriers. ACS Chem. Biol. *17*, 2559–2571. https://doi.org/10.1021/acschembio.2c00497.
185. Fransen, F., van Beek, A.A., Borghuis, T., Aidy, S.E., Hugenholtz, F., van der Gaast-de Jongh, C., Savelkoul, H.F.J., De Jonge, M.I., Boekschoten, M.V., Smidt, H., et al. (2017). Aged Gut Microbiota Contributes to Systemical Inflammaging after Transfer to Germ-Free Mice. Front. Immunol. *8*, 1385. https://doi.org/10.3389/fimmu.2017.01385.
186. Schober, P., Boer, C., and Schwarte, L.A. (2018). Correlation Coefficients: Appropriate Use and Interpretation. Anesth. Analg. *126*, 1763–1768. https://doi.org/10.1213/ANE.0000000000002864.
187. Oh, D.Y., Dowling, D.J., Ahmed, S., Choi, H., Brightman, S., Bergelson, I., Berger, S.T., Sauld, J.F., Pettengill, M., Kho, A.T., et al. (2016). Adjuvant-induced Human Monocyte Secretome Profiles Reveal Adjuvant- and Age-specific Protein Signatures. Mol. Cell. Proteomics *15*, 1877–1894. https://doi.org/10.1074/mcp.M115.055541.
188. van Haren, S.D., Pedersen, G.K., Kumar, A., Ruckwardt, T.J., Moin, S., Moore, I.N., Minai, M., Liu, M., Pak, J., Borriello, F., et al. (2022). CAF08 adjuvant enables single dose protection against respiratory syncytial virus infection in murine newborns. Nat. Commun. *13*, 4234. https://doi.org/10.1038/s41467-022-31709-2.

STAR★METHODS

KEY RESOURCES TABLE

REAGENT or RESOURCE	SOURCE	IDENTIFIER
Antibodies		
Viability dye, Fluorochrome LIVE/DEAD Aqua, at 1:500	Invitrogen	L34966
Anti-CD3, Clone 17A2, Fluorochrome Brilliant Violet 785, at 1:40	BioLegend	Cat# 100232; RRID: AB_2562554
Anti-CD4, clone RM4-5, Fluorochrome APC/Fire 750, at 1:160	BioLegend	Cat# 100568; RRID: AB_2629699
Anti-CD8, clone 53-6.7, Fluorochrome Brilliant UltraViolet 395 (BUV395), at 1:80	BD Biosciences	Cat# 563786; RRID: AB_2732919
Anti-CD44, clone IM7, Fluorochrome PerCP-Cy5.5, at 1:160	BioLegend	Cat# 103032; RRID: AB_2076204
Anti-IFNγ, clone XMG1.2, Fluorochrome Alexa Fluor 488, at 1:160	BioLegend	Cat# 505813; RRID: AB_493312
Anti-IL-2, clone JES6-5H4, Fluorochrome PE, at 1:40	BioLegend	Cat# 503808; RRID: AB_315302
Anti-TNF, clone MP6-XT22, Fluorochrome PE Cy7, at 1:160	BioLegend	Cat#506324; RRID: AB_2256076
Anti-IL-4, clone 11B11, Fluorochrome BV421, at 1:40	BioLegend	Cat# 504119; RRID: AB_10896945
Anti-IL-5, clone TRFK5, Fluorochrome BV421, at 1:160	BioLegend	Cat# 504311; RRID: AB_2563161
Anti-mouse IgG	Southern Biotech	Cat# 1036-05; RRID: AB_2794348
Anti-mouse IgG2a	Southern Biotech	Cat# 1081-05; RRID: AB_2736843
Anti-mouse IgG1	Southern Biotech	Cat# 1071-05; RRID: AB_2794426
Anti-RBD Fc chimera	R & D	Cat# 10499-CV-100; RRID: N/A
Anti-Human IgG Fc-HRP	Southern Biotech	Cat# 2048-05; RRID: AB_2795688
Biological samples		
Heparinized human whole blood (18–50 Y)	*Precision Vaccines Program*	NA
Heparinized human whole blood (>60 Y)	*Precision Vaccines Program*	NA
Heparinized human whole blood (>60 Y)	Brigham and Women's Hospital	NA
Chemicals, peptides, and recombinant proteins		
Heparin	American Pharmaceutical Partners Inc.	NDC71288-402-10
Urea	Sigma Aldrich	LC/MS grade
Ammonium bicarbonate	Sigma Aldrich	09830-1KG
Dithiothreitol	Sigma Aldrich	D9779-10G
Iodoacetamide	Sigma Aldrich	I1149-25G
Sera-Mag Speed Beads 65	Sigma-Aldrich	65152105050250
Sera-Mag Speed Beads 45	Sigma-Aldrich	45152105050250
HPLC-grade water	Sigma Aldrich	W5-4
Trypsin	Promega	V5117
Formic acid (LC/MS grade)	Thermo Scientific	A117-50
Recombinant RBD (R319-K529)	Nanishi et al.[130]	GenBank MN975262.1
Recombinant spike (M1-Q1208)	Nanishi et al.[130]	GenBank MN90894
Tetramethylbenzidine BD OptEIA	BD Biosciences	555214
Human ACE2	Sigma-Aldrich	SAE0064
Ammonium-Chloride-Potassium lysis buffer	Gibco	A10492-01
Acridine Orange/Propidium Iodide	Nexcelom	CS2-0106
PMA + ionomycin (at 1:500)	BioLegend	423301
Brefeldin (at 1:1000)	BioLegend	420601
Peptivator, wild type spike peptide pool	Miltenyi Biotec	130-126-700

(*Continued on next page*)

Continued

REAGENT or RESOURCE	SOURCE	IDENTIFIER
Cytofix/Cytoperm	BD	554714
Critical commercial assays		
Target 96 Inflammation panel	Olink	N/A
Target 96 Cardiometabolic panel	Olink	N/A
Target 96 Oncology III panel	Olink	N/A
Target 96 neurology panel	Olink	N/A
41-plex multiplex	Milliplex	HCYTOMAG-60K
Deposited data		
Human LC/MS proteomics data	ImmPort	SDY2630
Human PEA proteomics data	ImmPort	SDY2630
Human bead-based multiplex cytokine data	ImmPort	SDY2630
Experimental models: Organisms/strains		
BALB/c, female, >10 months	Envigo	BALB/cAnNHsd
BALB/c, female, 6–22 weeks	Envigo	BALB/cAnNHsd
SARS-CoV-2 (courtesy of Dr. Natalie Thornburg and CDC)	Nanishi et al.[130]	WA-1
Software and algorithms		
Skyline	MacLean et al.[148]	V20.2.1.315
R	R Development Core Team[149]	Versions 3.3.2 and 4.1.1
R Studio	RStudio Team[150]	Versions 1.3.1093, 2022.02.3 + 492, 2022.07.1 + 554 2023.03.1 + 446, 2023.06.1 + 524
AnnotationDbi	Pagès et al.[151]	1.62.2
ReactomePA	Yu and He[152]	1.44.0
DOSE	Yu et al.[153]	3.26.1
Ggraph	Pedersen[154]	2.1.0.9000
Geepack	Søren Højsgaard et al.[155]	1.3.9
mixOmics	Rohart et al.[156]	6.16.3
Limma	Ritchie et al.[157]	3.60.0
Plyr	Wickham[158]	1.8.7
dplyr	Hadley Wickham et al.[159]	1.0.9
reshape2	Wickham[160]	1.4.4
ggplot2	Wickham[161]	3.3.6
ggpubr	Kassambara[162]	0.4.0
ggfortify	Tang et al.[163] and Horikoshi et al.[164]	0.4.14
ggforce	Pedersen[165]	0.3.4
broom	Robinson et al.[166]	1.0.0
ggradar	Bion et al.[167]	0.2
tidyverse	Wickham et al.[168]	1.3.2
scales	Hadley Wickham[169]	1.2.0
FlowJo	BD	v.10.8.1
Biorender	Biorender.com	N/A
Other		
BNT162b2 monovalent wildtype SARS-CoV-2 vaccine overfill	Boston Children's Hospital pharmacy	EW0181

(*Continued on next page*)

Continued

REAGENT or RESOURCE	SOURCE	IDENTIFIER
Nexera Mikros	Shimadzu	N/A
Macrospin C18 plate	The Nest Group Inc.	SNS SS18VL
Capillary C18 Column	Shimadzu	227-32100-02
LCMS-8060 triple quadrupole mass spectrometer	Shimadzu	N/A
Nonheparinized capillary tubes	Drummond	1-000-1000
High-binding 96-well plate	Corning	9018
SpectraMax iD3 microplate reader	Molecular Devices	N/A
Nexcelom Cellometer K2	Nexcelom	N/A
LSRFortessa	BD Biosciences	N/A, custom

EXPERIMENTAL MODEL AND STUDY PARTICIPANT DETAILS

Human participant inclusion and exclusion criteria

Inclusion criteria included study participants >18 years of age who had responded to recruitment efforts, recruited between January-April, 2021, and who could give informed consent and who were willing and able to donate >75 mL blood. Participants were excluded if they had symptoms of an active infection (e.g., >38 C temperature), were recently immunized (14 days for non-live vaccines, 28 days for live attenuated), had donated >220 mL blood within the past 5 weeks, had taken anti-inflammatory medication that day, or taken immunosuppressants (e.g., corticosteroids, chemotherapy) within 3 months. Consenting participants had blood drawn, as summarized in the method details section, below.

Mice

BALB/c animals (BALB/cAnNHsd) were purchased from Envigo and housed at BCH. Female adult mice were used between 6 and 22 weeks of age, and aged female retired breeder mice were utilized within 43–59 weeks of age, a similar age group as used in other studies of immunosenescence,[170] communally housed with similarly aged animals. Adult mice were sex-matched to the availability of the aged female mice. Ear clipping enabled mouse tracking, and guided randomization balanced treatments across cages, to reduce variability. Mice were injected with 0.5, 1.0, or 5.0 μg of mRNA within monovalent wildtype BNT162b2, administered in 50 μL inoculum to the mouse's right hindlimb via intramuscular (IM) injection in either conscious or isoflurane-anesthetized mice. A prime-boost schedule was followed, separated by 14 days. Methodology for the evaluation of post-vaccination mouse serum for anti-spike immunity, antibody isotype, surrogate virus neutralization, and true neutralization as well as splenocyte dissection, dissociation, and $CD4^+$ and $CD8^+$ T cell stimulation, staining, and flow cytometry are summarized in the method details section, below.

METHOD DETAILS

mRNA vaccine

In vitro (human) and *in vivo* (murine) studies employed residual overfill, after removal of injectant for human immunization, of the monovalent wildtype Pfizer/BioNTech BNT162b2 mRNA vaccine from the BCH Pharmacy (February 2020-August 2022), within 12 h of vial puncture. Only monovalent BNT162b2 (encoding wildtype SARS-CoV-2 spike protein) was used.

Human participant sample processing

Heparinized whole blood was collected from adult (18-50Y), and older adult (elders, ≥60Y) study participants. Demographics, self-reported SARS-CoV-2 infection, and vaccination history were summarized in Table S1 for participant samples evaluated by LC/MS proteomics and multiplex, and in Table S2 for PEA evaluation. Clinical data on co-morbidities (e.g., obesity, corticosteroids, immunosuppression, cardiovascular disease, smoking, and other respiratory impacts) were not collected. Blood was drawn into a final 20 units/mL of clinical grade, pyrogen-free heparin (American Pharmaceutical Partners Inc.). WBA stimulation was performed as in[171,172] with a few modifications. Specifically, 125 μL blood was mixed 1:1 with RPMI 1640 (Gibco 11875-119) plus stimuli in 96-well U-bottom tissue culture plates (Becton Dickinson) and stimulated for 24 h in a 37°C humidified, 5% CO_2 incubator. Per-well stimulations of 0.002, 0.02, 0.2, 0.67, and 2.0 μg/mL of mRNA contained within BNT162b2 (0.1 μg mRNA/μL), corresponds to 0.002, 0.02, 0.2, 0.67, and 2%, % v/v, respectively. Cell-free supernatant was collected post-centrifugation (500g, 10 min), and stored at −80°C.

Evaluation of human culture supernatant

The impact of *in vitro* stimulation with BNT162b2 in the WBA was quantified by targeted plasma proteomics (liquid chromatography, mass spectrometry, LC/MS), proximity extension assay (PEA, 4x Olink Target 96 platforms) proteomics, and bead-based multiplex quantifying

inflammation and chemotaxis mediators. For proteomics, stimulated sample supernatants were randomized to avoid batch effects. Each assay, and methodology for analyte functional categorization is elaborated below.

Targeted plasma proteomics sample preparation

WBA samples were evaluated by LC/MS proteomics observing a dose-titration of BNT162b2-stimulated whole blood (WB). All chemicals and reagents were purchased at the highest purities available. Solvents used in this study were LC/MS grade and purchased from Fisher Chemicals (Thermo Fisher Scientific). Briefly, a volume of 10 μL of 10-fold diluted plasma was mixed with 60 μL of urea buffer (8M urea in 50 mM ammonium bicarbonate, Sigma Aldrich) and 15 μL of dithiothreitol buffer (DTT, 50 mM in urea buffer, Sigma Aldrich) before being incubated for 30 min on a thermomixer (800 rpm, room temperature, RT). The samples were alkylated with iodoacetamide buffer (375 mM in urea buffer, Sigma Aldrich) and incubated for 30 min (800 rpm, RT and dark). A volume of 10 μL of DTT buffer was added to quench the alkylation. The samples were transferred to the SP3 beads mixture (Sera-Mag SpeedBeads, 1:1 v/v, GE Healthcare) previously washed with high-performance liquid chromatography (HPLC)-grade water (Sigma Aldrich) at a 1:10 protein to bead ratio. A volume of 150 μL of absolute ethanol (Superlco) was added and incubated 15 min on a thermomixer (1,000 rpm at RT). The samples were placed on the magnetic rack and then the clear supernatant was removed. The beads were washed three cycles in 200 μL 80% ethanol. After the final washing step, the samples were trypsinized with 100 μL of trypsin buffer (Promega, 20 μg/mL in 50 mM ammonium bicarbonate) and placed on thermomixer (1,000 rpm, 2 h, 37°C). After digestion, samples were centrifuged to pull down the liquid and placed on magnetic rack to collect the supernatant and were acidified with 2% v/v formic acid in HPLC water. The C18 cleanup was performed using a 96-well MACROSPIN C18 plate (TARGA, The NestGroup Inc.) and the tryptic peptides were eluted off the C18 particles using 40% ACN/0.1% FA. The samples were then dried and stored at −20°C until LC/MS analysis. The samples were analyzed using an LC system (Nexera Mikros, Shimadzu) equipped with Capillary C18 column (0.2 × 100mm, 2.7 μm particle diameter, Shimadzu) coupled online to an LCMS-8060 triple quadrupole mass spectrometer instrument (Shimadzu). From each sample, 1 μg peptide quantity was separated using a non-linear gradient over 15-min run time operated at 10 μL/min (5% solvent B for 0.2 min; 5 to 40% B for 10.3 min; 85% B for 1.5 min and 5% for 3 min). The final scheduling method was performed using the following parameters: 1.2 s of maximum loop time with minimum dwell time of 2 msec and pause time of 1 msec, Q1 and Q3 resolution set at the 'unit' level.

Proximity extension assay (PEA)

To broaden the range of proteins measured, supernatants from human *in vitro* WBA assays were also evaluated by a Proximity Extension Assay (PEA) with Olink technology, as in,[173] following manufacturer recommendations. An n of 5 adult and 5 aged participants were evaluated, and an *n* 5 adult and 4 elder passed blinded quality control measures. Of note, due to quality control warnings, one elder research participant was removed from the original *n* 5, according to the manufacturer's sample-blinded quality control recommendations. These participant samples were a subset of those investigated by LC/MS proteomics. Samples were selected while blinded to outcomes and were chosen to reduce the number of sample freeze thaw cycles. Proteins were labeled with a mixture of antibodies containing pairs of antibodies tagged with a DNA barcode that were able to recognize the same protein. Antibodies binding to the same target, in close proximity, have DNA tag hybridization, undergo DNA polymerase-dependent extension, subsequent PCR amplification, and next generation sequencing (NGS). The dual antibody binding and PCR amplification resulted in high specificity and sensitivity to evaluate normalized protein expression (NPX). Four Target 96 panels (Inflammation, Cardiometabolic, Oncology III, and Neurology) were assayed by Olink under a service agreement. PEA assay-quantified proteins were labeled with the platform name (Inflammation, 'inflam'; Oncology, 'onco'; Neurology, 'neuro'; Cardiology III, 'cardio'). A total of 368 proteins were evaluated while blinded to age group, and analyses were performed at BCH. For conditions comparing LNP-stimulations between age groups baseline-normalization via subtracting vehicle control from LNP-stimulated conditions to reduce inter-assay variability and were evaluated for differential (up/down regulation) normalized protein expression in samples stimulated with 2 μg/mL of encapsulated BNT162b2 mRNA against vehicle (RPMI) controls. PEA heatmap analysis was unsupervised to evaluate if patterns of LNP-induced proteins could differentiate stimulated from non-stimulated in adults and elders. Euclidean-clustering was applied to evaluate BNT162b2-stimulated adult clustering and elder non-clustering. The top 100 differentially expressed proteins were converted to Entrez IDs with the AnnotationDbi package and then enrichment analysis was performed with ReactomePA. Plotting of network interactions involved cnetplot and ggraph. Network analysis nodes were sized by the number of contributing proteins.

Bead based multiplex

Human samples from WBA were also evaluated by a bead-based multiplex platform measuring 41 analytes (Milliplex HCYTOMAG-60K) following the manufacturer's recommendations and excluding samples with insufficient bead counts (requiring $\geq$30 beads/analyte).

Functional categorization of analytes

Selection of individual significantly induced proteins increases the risk of interpretation bias due to analyte polyfunctionality and the potential of false positives. We augmented the classical approach of individual analyte interpretations from multiplex assays by additionally analyzing based on functional categorization to evaluate if age significantly interacted with each function. Immunosenescence could be driven by differential production of analytes capable of polarizing naive T cells toward $CD4^+$ T helper cell (T_H) 1, T_H2, T_H17, and T_{reg} differentiation, and those supporting chemotaxis, hematopoiesis, and/or associated with secondary effects of vaccine (e.g., trained immunity, nonspecific

effects). T_H1 polarized immune responses can trigger effective intracellular pathogen responses,[133] including $CD8^+$ T cell-mediated immunity,[134] B cell class switching[98,99] and induction of T_{FH}-like activity for effective B cell responses in the absence of T_{FH}.[135] T_H2 responses can support Ab production but can bias toward IgE Ab class switching with potential age-dependent differences.[98,174] T_H17 has been associated with B cell differentiation and class switching to IgA,[175–177] with increased mucosal immunity.[178] Chemokine responses are critical for mounting an effective immune response,[179] through both initial recruitment of monocytes to the vaccination site, and subsequent chemotaxis of mature antigen-presenting cells (APC) to the draining lymph node.[85–88] T_{reg} can restrain germinal center reactions.[130,180] Hematopoiesis-associated factors could be important immunoregulators, as impaired hematopoiesis has been associated with reduced vaccine responsiveness in the aged.[181,182] mRNA vaccines may also induce trained immunity.[38,183] Impact of age on each function was evaluated through a targeted multiplex cytokine and chemokine assay measuring 41 predominantly polyfunctional analytes.

A literature review informed classification of each of the 41-plex measured analytes into the functional categories of T_H1, T_H2, T_H17, and T_{reg} polarizing, and chemokine, hematopoiesis, or vaccine associated trained immunity inducing functions. Particular attention to differentiate polarizing activity from analytes that were produced by polarized cells was performed. This review included various gene ontology (GO) terms, including 'T cell differentiation' (GO: 0030217, sub-divided to T_H1 or T_H2 or T_H17 polarizing), 'T-helper 17 cell lineage commitment' (GO: 0072540), 'regulatory T cell number' (GO: 0045066), 'Chemokine' (GO: 0032602), 'Chemotaxis' (GO 0006935), and 'Hematopoiesis' (GO: 0030097). Supplemental targeted searches of each function, and "polarizing" or "polarized," in the case of T_H-polarizing activity, in the *Google Scholar* database between Aug-Oct 2021. Evidence from human sources was prioritized but supplemented with murine where human observations were not available. Categorization into the $CD4^+$ T cell polarizing capacities required evidence of being required for polarization, or inducing polarization itself, rather than being induced by a polarized cell. The other evaluated functions included direct and indirect chemokine activity, hematopoiesis support or induction, and mediating secondary effects of vaccines.

Murine SARS-CoV-2 specific antibody evaluation

At 14, 28, 42, and 210 days post-prime immunization animals were anesthetized under 3% isoflurane and had 100-200 μL of blood collected by retroorbital bleed into non-heparinized glass capillary tubes (Drummond Cat. 1-000-1000). Prompt expelling of blood into microcentrifuge tubes was followed by allowing samples to clot. Blood was centrifuged within 2 h (1500g, 7.5 min), transferred to new microcentrifuge tubes, recentrifuged, and serum was aliquoted for storage at −80°C.

Anti-spike and anti-RBD titers were evaluated by ELISA as in.[130] In brief, flat-bottomed high-binding 96-well Corning plates (NY, catalog 9018) were coated with 25 ng per well of SARS-CoV-2 wildtype sequence of recombinant RBD (GenBank MN975262.1, amino acids R319-K529) or 50 ng per well of recombinant spike (GenBank MN90894, amino acids M1-Q1208) glycoprotein. These proteins were produced with constructs consisting of a *TwinStrepTag*, an HRV3C cleavage site, and an 8XHisTag C-terminal modification from Aaron G. Schmidt from the Ragone Institute, and Barney S. Graham from the NIH Vaccine Research Center, respectively. Overnight incubation at 4°C was followed by 0.05% Tween 20 in PBS-wash of plates, with subsequent 1% bovine serum albumin (BSA) blocking for 1 h at RT. Serum samples were initially diluted 1:100 then 4-fold serially diluted to a dilution factor of 1.05E8, followed by incubation in the pre-coated plate for 2 h at RT. Following 3 washes a 1 h RT incubation with horseradish peroxidase (HRP)-conjugated goat anti-mouse IgG, IgG2a, or IgG1 (Southern Biotech respective cat. 1036-05, 1081-05, 1071-05) was performed. Following 5 × 0.05% Tween 20 in PBS washes, RT tetramethylbenzidine (TMB, BD OptEIA substrate solution from BD Biosciences) was added for 5 min, then stopped with sulfuric acid, 2N H_2SO_4. Optical density (OD) was determined at 450 nm in a SpectraMax iD3 microplate reader (Molecular Devices). Assignment of antibody titer was calculated from the final dilution where TMB was over 3x background. Any value below 3x background was assigned half the initial serum dilution of 100.

Murine surrogate virus neutralization titer (sVNT) evaluation

Murine sera were evaluated using a previously as in.[130] Specifically, flat-bottomed high-binding 96-well Corning plates (NY, catalog 9018) were incubated with 100 ng recombinant human angiotensin-converting enzyme 2 (hACE2, Sigma-Aldrich) in PBS, per well, overnight at 4°C. Following 3 x washes with 0.05% Tween 20 in PBS, plates were blocked for 1 h RT with 1% BSA. Sera were initially diluted 1:160, then incubated with 3 ng of RBD conjugated with an Fc fragment of IgG (RBD-Fc) for 1 h at RT. Sample mixtures were transferred to the hACE2 coated plates alongside the positive control (PC) of non-serum, RBD alone and the negative control (NC) of 1% BSA in PBS alone. After a 1 h RT incubation, 3 x washes with 0.05% Tween 20 in PBS were incubated with anti-human IgG Fc with HRP-conjugation (Southern Biotech). After an additional 5 x washes plates were TMB-developed, H_2SO_4 stopped, and read at 450 nm, as in the Ab evaluation. Percent inhibition was evaluated by calculating (1 – (Sample OD - NC OD)/(PC OD – NC OD)) x 100.

Live SARS-CoV-2 virus neutralization test

Murine samples were evaluated as in.[123,124] Specifically, processing and scoring of samples were performed randomized and blinded to animal treatment. Sera were heat-inactivated at 56°C for 30 min to deactivate complement. Once equilibrated to RT, samples were processed in duplicate to evaluate neutralization titer. Samples were initially diluted 1:20, followed by a 1:2 serial dilution resulting in a 12-dilution series with each well containing 60 μL. Dilutions employed Dulbecco's Modified Eagle Medium (DMEM, Quality Biological) supplemented with 10% (v/v) heat-inactivated fetal bovine serum (HI-FBS, Gibco), 1% penicillin/streptomycin (v/v, Gemini Bio-products) and 1% L-glutamine (v/v, 2mM final concentration, Gibco). Dilution plates were transported to biosafety level (BSL)-3 where 60 μL of diluted SARS-CoV-2 inoculum (WA-1 strain, courtesy of Dr. Natalie Thornburg, and the CDC) was added to each well with serum, resulting in a multiplicity of infection of 0.01, corresponding to 100 pfu/well. Each plate had a non-treated virus-only control and a mock-infection well to establish cytopathic effects. After 1 h

incubation at 37°C with 5% CO_2, 100 μL of sample-virus complexes were transferred to a 96-well plate with confluent (~1e4) Vero Transmembrane serine protease 2 (TMPRSS2) cells. Incubation of cells with virus permitted evaluation of cytopathic effect (CPE) after 72 h where the first dilution displaying CPE was set as the minimum sample dilution needed to neutralize >99% of the SARS-CoV-2 tested.

Murine splenocyte evaluation

Assessment of cell mediated immunity in adult and older mice made use of CO_2-euthanizing mice between days 39 and 41 post-prime immunization with prompt aseptic collection of spleens at 4°C in 1 mL of RPMI 1640 (Gibco 11875-119) with 10% HI-FBS (HyClone, GE Healthcare) that was 0.22 μm-filtered. Mouse euthanasia was batched to reduce the amount of time (<10 min) that the spleen was within the mouse without active circulation. Downstream splenocyte processing was batched with no more than 3 mice at a time to reduce the amount of time that cells were without circulatory support and off ice. Aseptic dissection included care to dissect away pancreatic tissue, which otherwise can impact cell viability. Splenocytes were dissociated by gently pressing the spleen through a 70 μm cell strainer (Falcon cat. 352350) using the plastic portion of a 3 mL syringe's plunger, aseptically removed from its wrapper. After twice rinsing the strainer and plunger with 1 mL cold RPMI (4°C), an additional 16 mL rinse of the strainer alone was performed. Following centrifugation (315g for 10 min) supernatant was decanted so that ≤200 μL of liquid remained, cells were resuspended in residual volume, and red blood cells (RBCs) lysed with 1 mL of RT Ammonium-Chloride-Potassium (ACK) lysis buffer (Gibco, Cat A10492-01, Waltham, MA) for exactly 2 min at RT. Osmotic lysis was neutralized immediately and cells washed with 25 mL cold RPMI, passed through a new 70 μm cell strainer, centrifuged, resuspended in RPMI +10% HI-FBS, and cells were counted by dual Acridine Orange/Propidium Iodide (AOPI) staining (Nexcelom Cellometer K2, CS2-0106). To restore basal activity levels, cells were plated at 2 x 10^6 total cells/well in 200 μL in a 96 well U-bottom plate, then rested overnight (37°C, 5% CO_2) in T cell media consisting of RPMI 1640 (Gibco, Waltham, MA) supplemented with 10% HI-FBS (HyClone, Cytiva), 100 U/mL Penicillin and 100 mg/mL Streptomycin (Gibco, Waltham, MA), 55 mM 2-mercaptoethanol (Gibco, Waltham, MA), 60 mM non-essential Amino Acids (Gibco, Waltham, MA), 11 mM HEPES (Gibco, Waltham, MA), and 800 mM L-Glutamine (Gibco, Waltham, MA).

Flow cytometry of murine splenocytes

Following overnight rest, processed splenocytes were stimulated with SARS-CoV-2 wild type spike peptide pools (PepTivator, #130-126-700, Miltenyi Biotec) at 1 μg/mL in the presence of anti-mouse CD28/49days (1 μg/mL, BD) and brefeldin A (5 μg/mL, BioLegend). After 6h of stimulation, cells were washed twice with PBS and blocked with Mouse Fc Block (BD Biosciences) according to the manufacturer's instructions. After blocking, cells were washed once with PBS and stained with Aqua Live/Dead stain (Life Technologies, Carlsbad, CA) for 15 min at RT. Following two additional PBS washes, cells were resuspended in 100 μL of FACS buffer (PBS supplemented with 0.2% BSA (Sigma-Aldrich)) containing mouse specific cell surface markers for flow cytometry. Markers included anti-mouse CD44 PerCP-Cy5.5, CD3 BV785, CD4 APC/Fire750 and CD8 BUV395. Clone and manufacturer in the customized nine color, 10 marker flow cytometry panel are documented in the Key Resources table, and as in.[184] Cells were incubated with surface markers for 30 min at 4°C. Cells were PBS-washed and fixed/permeabilized with a Cytofix/Cytoperm kit (BD, #554714), following manufacturer's recommendations. Cells were washed in 1X perm/wash solution and subjected to intracellular staining (30 min at 4°C) using a cocktail of the following Ab: anti-mouse IFNγ Alexa Fluor 488, TNF PE Cy7, IL-2 PE, IL-4 BV421 and IL-5 BV421 in 1X perm/wash solution. Finally, cells were washed in PBS and fixed in PBS containing 1% paraformaldehyde (Electron Microscopy Sciences, Hatfield, PA) for 20 min at 4°C. After two final washes in PBS, the cells were resuspended in PBS and stored at 4°C until acquisition. Samples were acquired on a BD LSRFortessa (BD Biosciences; San Jose, CA) configured with blue (488 nm), yellow/green (568 nm), red (640 nm), violet (407 nm), and ultraviolet (355 nm) lasers using standardized good clinical laboratory practice procedures to minimize variability of data generated. Analysis was performed using FlowJo software, v.10.8.1 according to the gating strategy outlined in Figure S6. Positive gates for each cytokine were determined using fluorescence minus one (FMO) controls for IFNγ, TNF, IL-2, and IL-4/5 where all antibodies were used except the targeted one. Population gating was performed blinded to treatment group. PBS group samples were stimulated with mitogen (BioLegend, #423301 at 1:500) for 6 hr as positive controls for Th1 and Th2 signatures. Baseline $CD4^+$ T cell activation can be impacted by inflammaging,[185] therefore we performed baseline normalization by evaluating adult and aged mice for their fold induction of $CD4^+$ T cell responses from immunized mice over the average age-matched vehicle control.

QUANTIFICATION AND STATISTICAL ANALYSIS

Proteomic, multiplex, and murine immunogenicity data were analyzed and graphed using R (versions 3.3.2 and 4.1.1). Raw data from LC/MS proteomics were exported into *Skyline* software (v20.2.1.315)[148] for peak area and retention time refinement. PEA was evaluated by Olink, blinded to treatment, with normalized protein expression (NPX) data sent to BCH. Missing data (e.g., below lower limit of quantification (LLOQ) or were NA (no data)) were replaced with the limit of quantification values as recommended by Olink. 39 of 368 PEA-measured analytes had >60% missing data, necessitating removal before analyses. LC/MS proteomic responses were expressed as fold change of stimulated samples divided by matched controls calculated for baseline adjustment. LC/MS titratable up- and down-regulated responses were evaluated by generalized estimating equations generalized linear model (GEEGLM) analysis,[39–41] leveraging multiple stimulation concentrations into 1 measure to determine if stimulation and age interacted and impacted analyte levels. Specifically, the 'geepack' package in R was used to evaluate log fold change (logFC) of analyte induction in BNT162b2 stimulated over paired RPMI control (logFC) against ('~') the treatment concentration (μg/mL of mRNA in BNT162b2), with an added evaluation ('+') of the interacting effect of participant age group (adult or elder) and ('*') categorized analyte function (e.g., T_H1-polarizing or not). This assessment was repeated for each functional role evaluated. PEA

assays did not have the same spread of stimulation doses as LC/MS and were evaluated by a moderated T-test between the WBA stimulated with 2 μg/mL of mRNA encapsulated in BNT162b2, versus vehicle (RPMI) control. Multilevel principal component analysis on NPX was performed using the PCA function in mixOmics 6.16.3 package. PEA quantified responses were evaluated with Spearman's correlation analyses.

Bead-based multiplex samples were evaluated by linear modeling testing for dose dependency of each analyte in non-transformed pg/mL. Fold change (FC) of stimulated sample divided by a matched RPMI control was performed, then $\log_{10}$ transformed. GEEGLM evaluated the interacting effect of age on various cytokine functions with non-interacting effect of stimulation by evaluating fixed effects of 'BNT162b2 stimulation amount' and 'age group' on LogFC of analyte induction, as above. Exponentiation of the point estimate for each fixed effect allowed for an interpretation of effects as percent increase/decrease, with confidence intervals determined by adding or subtracting 1.96 multiplied by the standard error prior to exponentiation. Data were presented by radar plot per-functional category, filtering for only the analytes associated with each function.

Evaluation of murine samples was based on Shapiro-Wilk test for normality then T-test for normally distributed, or Kruskal-Wallis and Wilcoxon rank-sum tests for non-normally distributed data. Locally estimated scatterplot smoothing (loess) was selected to model best-fit lines between correlations. Spearman correlation test of a monotonic relationship between murine IgG and SVNT was performed due to nonnormal distribution[186] of anti-spike IgG, enabling evaluation of whether an increase in anti-spike IgG would correspond to an increase in SVNT between age groups.

Statistical significance was denoted graphically by *$p < 0.05$, **$p < 0.01$, ***$p < 0.001$, and ****$p < 0.0001$. Sample size was selected based on sample and kit availability (collected in the midst of the SARS-CoV-2 public health emergency), triggering evaluation upon sufficient sample accumulation based on previous experience in modeling age-dependent differences by LC/MS and bead-based multiplex approaches ($n \geq 6$ and 10 per age group),[35,187,188] and based on PEA kit availability (n 5 per age group) for exploratory investigation. Specifically, in Figure 1, sample sizes were (A-B) n = 10–14 and (C-D) n = 4–5, with significance by (A-B) GEEGLM analysis with nominal p-value <0.05, and (C-D) paired moderated T-test reporting nominal p-values <0.05. Horizontal dotted lines represent -log10(0.05), and non-significant (NS) findings were visualized as gray circles. In Figure 2, Sample sizes were (A-B) n = 10–14 and (C-F) n = 4–5. Evaluation of significance was by (B) GEEGLM with nominal p-values, (C) paired moderated T-test with adjusted p-values <0.05, and (D) Spearman's correlation with nominal p-values. (B, C) Horizontal dotted lines represent -log10(0.05). In Figure 3, analyses were performed with (A) Shapiro-Wilk then Wilcoxon rank-sum tests evaluating paired analyses. (B, C) Age group comparisons were evaluated by 1-sided unpaired T-tests on log-transformed fold-change. Concentration-dependent induction was evaluated with linear modeling of log10-transformed analyte levels, with R^2 and significance annotated by age. Boxplots display median with interquartile range, with n = 12–14. In Figure 4, sample sizes were n = 12–14, with significance evaluated by 1-sided T-test hypothesizing induction. In Figure 5, sample sizes were n = 5–10. Significance was determined by Shapiro-Wilk, Kruskal-Wallis, then (A) one-sided Wilcoxon rank-sum hypothesizing vaccine-associated induction compared to vehicle control, and two-sided Wilcoxon rank-sum test comparing younger adult to aged mice, (B) two-sided Wilcoxon rank-sum test, and (C) two-sided T-test. The graphics for figures and the graphical abstract were created with BioRender.com.

Data management and deposition

Data quality control (QC) was performed for each platform by the endpoint laboratories following assay-specific outputs described above. Data quality assurance (QA) by the *Precision Vaccines Program* Data Management & Analysis Core (DMAC) entailed verifying application of QC criteria within a centralized cloud-based infrastructure. Deidentified quality assured human data from this manuscript is publicly deposited in the NIH/NIAID-supported repository *Immport:* SDY2630.

Ethics study approval statement

Experiments were performed under institutional and national guidelines. Volunteer study participants donated blood samples following informed consent, approved by Boston Children's Hospital (BCH) Institutional Review Board (IRB, X07-05-0223, IRB-P00013867) and Biosafety (IBC-P00001416), and Brigham and Women's Hospital IRB 2013P002473). Animal procedures were approved by the Institutional Animal Care and Use Committee (00001573), with supervision from the Department of Animal Resources at BCH.